


Prospects for the determination of fundamental constants with beyond-state-of-the-art uncertainty using molecular hydrogen ion spectroscopy

S. Schiller

Institut für Experimentalphysik, Heinrich-Heine-Universität Düsseldorf, 40225 Düsseldorf, Germany

J.-Ph. Karr

*Laboratoire Kastler Brossel, Sorbonne Université, CNRS, ENS, Université PSL, Collège de France, 4 Place Jussieu, 75005 Paris, France
and Université d'Evry-Val d' Essonne, Université Paris-Saclay, Boulevard François Mitterrand, 91000 Evry, France*

 (Received 27 December 2023; revised 2 March 2024; accepted 22 March 2024; published 23 April 2024)

The proton, deuteron, and triton masses can be determined relative to the electron mass via rovibrational spectroscopy of molecular hydrogen ions. This has to occur via comparison of the experimentally measured transition frequencies and the *ab initio* calculated frequencies, whose dependence on the mass ratios can be calculated precisely. In precision experiments to date (on HD^+ and H_2^+), the transitions have involved the ground vibrational level $v = 0$ and excited vibrational levels with quantum numbers up to $v' = 9$. For these transitions, the sensitivity of the *ab initio* frequency to the high-order QED contributions is correlated with that to the mass ratios. This prevents an efficient simultaneous determination of these quantities from experimental data, so the accuracy of the mass ratios is essentially limited by the theoretical uncertainty. Here we analyze how the accuracy of mass ratios may be improved by providing experimental transition frequencies between levels with larger quantum numbers, whose sensitivity to the mass ratio is positive rather than negative, or close to zero. This allows the unknown QED contributions and involved fundamental constants to be much more efficiently determined from a joint analysis of several measurements. We also consider scenarios where transitions of D_2^+ are included. We find these to be powerful approaches, allowing us in principle to reach uncertainties for the mass ratios approximately three orders smaller than reported by CODATA 2018. Improvements by a factor of 3.5 for the Rydberg constant, and 11 (14) for the proton (deuteron) charge radius, are also projected.

DOI: [10.1103/PhysRevA.109.042825](https://doi.org/10.1103/PhysRevA.109.042825)

I. INTRODUCTION

The precision spectroscopy of the molecular hydrogen ion (MHI) HD^+ has made significant progress in the past few years. The combination of recently obtained experimental [1–5] and theoretical results [6] on the transition frequencies permits extracting one fundamental constant, the reduced proton-deuteron mass relative to the electron mass μ_{pd}/m_e . The current uncertainty from MHI spectroscopy, $u([\mu_{pd}/m_e]_{\text{expt,HD}^+}) \simeq 2.5 \times 10^{-8}$ [5,7], is competitive with direct mass measurements using Penning traps [8–11]. The accuracies of some of the experimentally determined transition frequencies are already higher than those of the theoretical predictions. Hence, the latter limit the accuracy of the determination of μ_{pd}/m_e . The theoretical uncertainty is dominated by unknown high-order QED contributions [6].

The question arises as to what the fundamental limitations are to the attainable uncertainties in the determination of the mass ratios, as well as of other constants, using any possible future result of MHI spectroscopy. The question was first addressed in an earlier analysis [12], where different measurement scenarios were considered. A scenario that included three HD^+ transitions and two H_2^+ transitions (assumed to have been measured with fractional uncertainties 1×10^{-12}), with no other experimental input data, and assumed 3×10^{-12} theory uncertainty resulted in a proton-electron mass-ratio uncertainty $u(m_p/m_e) \simeq 1.5 \times 10^{-8}$.

In the present study, we seek to break the correlation between the theoretical uncertainties of the transition frequencies due to uncalculated terms. The existence of this correlation was first emphasized in Ref. [12]. Alighanbari *et al.* [5] observed that the correlation is partially removed when computing ratios of theoretical transition frequencies between levels of not-too-disparate vibrational quantum numbers. The agreement between theoretical and experimental ratios exhibits a particularly small combined uncertainty.

Two different approaches are used in our study: (i) a simplified approach, in which the unknown QED contributions are treated as a single parameter to be determined by solving a system of linear equations, and (ii) a least-squares adjustment, similar to CODATA [13] and Ref. [7], where QED contributions to the different transition frequencies are treated as adjustable parameters. We also propose to include qualitatively different vibrational transitions in the measurement program and discuss several scenarios, i.e., sets of transitions measured on different MHIs.

Figure 1 summarizes the current situation and presents one main idea of this paper. The figure displays, for six transitions of HD^+ , the correlation between the unknown (uncalculated) QED contribution and the mass-ratio value deduced from requiring the theoretical frequency to match the experimental frequency. The four transition frequencies measured to date (green, light blue, brown, and gray) have a similar relationship between mass uncertainty and QED uncertainty: The bands

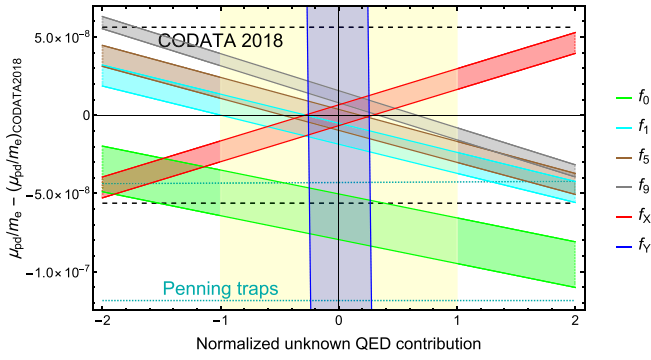


FIG. 1. Determination of the nuclear-electron mass ratio of HD^+ from single transition frequencies. Shown are four already measured transitions f_0 , f_1 , f_5 , and f_9 and two hot-band transitions considered for future measurement, $X:(v=9, N=1) \rightarrow (v'=18, N'=0)$ and $Y:(7, 1) \rightarrow (15, 0)$. Here f_X (red) is a positive-mass-sensitivity transition and f_Y (blue) is a suppressed-mass-sensitivity transition. Note that the band slope is similar for f_0 , f_1 , f_5 , and f_9 because the abscissa is the normalized QED contribution $\Delta_{\text{nuc,QED}}/0.32$ [see Eq. (14)]. The width of each band takes into account (i) the uncertainty of the theoretical transition frequency due to the uncertainty of the Rydberg constant and the uncertainties of the rms charge radius of the proton and deuteron, (ii) the uncertainty of the experimentally measured frequency, and (iii) the uncertainty of the hyperfine structure theory. For the four measured transitions, the experimental results $f^{\text{(expt)}}$ and theoretical results with CODATA 2018 constants $f_{2018}^{\text{(theor)}}$ have been used in the plot. For the proposed transitions (red and blue bands) we have assumed a hypothetical perfect match $f^{\text{(expt)}} = f_{2018}^{\text{(theor)}}$, experimental uncertainties $u(f_X^{\text{(expt)}}) = u(f_Y^{\text{(expt)}}) = 0.3$ kHz, and spin theory uncertainty 0.035 kHz. The yellow shaded range indicates the estimated normalized uncertainty of the unknown QED contribution to the theoretical transition frequency, stemming from the three contributions $u(\delta f_{\text{QED},1})$, $u(\delta f_{\text{QED},2})$, and $u(\delta f_{\text{QED},3})$ (see the text for details). The horizontal black dashed lines indicate the ± 1 standard uncertainty interval of the value of μ_{pd}/m_e according to CODATA 2018. The dark cyan dotted lines represent the ± 1 standard uncertainty interval of μ_{pd}/m_e derived from Penning trap measurements. It is computed from the uncertainties of the atomic mass of the electron [8] (modified as in [14]), of the atomic mass of the deuteron [10], and of the proton-deuteron mass ratio [11].

have similar slopes. Considering each measured frequency independently, as well as the estimated uncertainty of the QED contributions (yellow band), we can derive a value for the mass ratio with uncertainty $u([\mu_{pd}/m_e]_{\text{expt,HD}^+}) \simeq 2.5 \times 10^{-8}$. This is substantially determined by the QED uncertainty.

The similar band slopes imply that even when the four transitions are taken together, they are not particularly effective in reducing the uncertainty of the mass ratio. If, however, a suitably chosen additional transition frequency is introduced, whose slope is qualitatively different (f_X , red band), then a simultaneous determination of both the mass correction and the QED correction with reduced uncertainty becomes possible. This will be discussed in detail in the following.

A. Theoretical transition frequencies

We consider only the so-called spin-averaged rovibrational frequencies. This is reasonable since it has been shown

theoretically that the contribution of hyperfine energies can be completely eliminated by measuring the complete set of hyperfine components of a transition and then applying a sum rule [15]. A demonstration was recently given in [16]. The *ab initio* theory of the spin-averaged frequency is well developed [6]. A spin-averaged theoretical frequency may be decomposed as

$$f^{(\text{theor})} = f_{\text{nr}}(R_\infty, \{m_i/m_e\}) + \delta f_{\text{QED}}(R_\infty, \alpha, \{m_i/m_e\}) + \delta f_{\text{nuc}}(\{r_i\}) + \delta f_{\text{nuc,ho}}, \quad (1)$$

where the important dependences on fundamental constants are indicated. Here R_∞ is the Rydberg constant, m_i is the mass of a nucleus (proton, deuteron, or triton), m_e is the electron mass, α is the fine-structure constant, and r_i is the charge radius of a proton, deuteron, or triton. In addition, all terms in the equation are functions of the vibrational and rotational quantum numbers of the lower (v, N) and upper (v', N') rovibrational levels; they will be indicated explicitly below. The first term f_{nr} is the nonrelativistic transition frequency, arising from the solution of the three-body Schrödinger equation. The second term δf_{QED} contains all energy corrections due to relativistic and QED effects. The third term is the leading-order finite-nuclear-size shift. Finally, the fourth term $\delta f_{\text{nuc,ho}}$ contains small nuclear corrections of higher order, whose dependences on fundamental constants may be neglected. The fundamental constants displayed in the equation above represent the dominant dependences.

MHI spectroscopy can be exploited to determine one or more of the above fundamental constants from the comparison of a set of experimentally measured transition frequencies $\{f_k^{\text{(expt)}}\}$ and their theoretical counterparts $\{f_k^{\text{(theor)}}\}$. We therefore first discuss qualitatively the impact of theoretical uncertainties and uncertainties of the fundamental constants on the four terms of $f_k^{\text{(theor)}}$.

B. Uncertainty of the theoretical prediction

To begin with, we consider the uncertainties stemming from the involved fundamental constants. All terms in Eq. (2) are proportional to the Rydberg constant; however the impact of its current uncertainty (reported by CODATA 2018 [14]) is mainly on the first term, since the second largest term δf_{QED} is approximately 5×10^4 times smaller than the first. The uncertainty of the mass ratios therefore also affects mostly the first term. Since we actually wish to determine mass ratios more accurately than provided by CODATA 2018, the sensitivity of f_{nr} to the mass ratios, i.e., the partial derivatives $\partial f_{\text{nr}}/\partial(m_i/m_e)$, are important quantities. They have been computed in a number of works, e.g., [17,18]. Since the fine-structure constant does not enter f_{nr} except via R_∞ , its current uncertainty is not relevant in f_{nr} .

The third term δf_{nuc} is equal to the difference of the finite-nuclear-size shifts in the upper and lower levels. The shift of each energy level is proportional to the expectation value of the delta potential $V_{\delta,i} = \delta(\mathbf{r}_{e,i})$ of the electron at nucleus i , i.e., to the probability density at the nucleus. Here $\langle V_{\delta,i} \rangle$ is expressed in atomic units. Its values can be accurately calculated. The nuclear-size shift for a heteronuclear MHI is

TABLE I. Some transitions of HD^+ and their properties. The first one is a rotational transition and the others are vibrational transitions. The last four entries are hot-band transitions. Transition 5 is the only one listed that has a positive s . Here $\lambda = \mu_{pd}/m_e$, $V_\delta \equiv V_{\delta,pd}$, and $\Delta V_\delta \equiv \Delta V_{\delta,pd}$.

No.	Transition (v, N) \rightarrow (v', N')	Frequency		s $\partial f_{\text{nr,a.u.}}/\partial \lambda$	V $\langle V_\delta \rangle_{v',N'} - \langle V_\delta \rangle_{v,N}$	ΔV $\langle \Delta V_\delta \rangle_{v',N'} - \langle \Delta V_\delta \rangle_{v,N}$
		f (THz)	$f_{\text{nr,a.u.}}$			
1	(0, 0) \rightarrow (0, 1)	1.31	0.000200	-1.611×10^{-7}	-0.0003698	2.0×10^{-10}
2	(0, 0) \rightarrow (1, 1)	58.6	0.00891	-3.526×10^{-6}	-0.009850	-6.8×10^{-6}
3	(0, 0) \rightarrow (5, 1)	260	0.0395	-1.363×10^{-5}	-0.04187	-0.000057
4	(0, 3) \rightarrow (9, 3)	415	0.0631	-1.816×10^{-5}	-0.06460	-0.00018
5	(9, 1) \rightarrow (18, 0)	208	0.0316	8.272×10^{-6}	-0.02868	-0.0043
6	(7, 1) \rightarrow (15, 0)	237	0.0360	-3.113×10^{-8}	-0.03373	-0.00095
7	(9, 1) \rightarrow (13, 0)	118	0.0180	-1.027×10^{-7}	-0.01671	-0.00036
8	(5, 1) \rightarrow (13, 0)	278	0.0422	-5.242×10^{-6}	-0.04059	-0.00049

given by [19]

$$\delta f_{\text{nuc}} = 2cR_\infty(2\pi/3)a_0^{-2} \left[r_1^2 (\langle V_{\delta,1} \rangle_{v',N'} - \langle V_{\delta,1} \rangle_{v,N}) + r_2^2 (\langle V_{\delta,2} \rangle_{v',N'} - \langle V_{\delta,2} \rangle_{v,N}) \right], \quad (2)$$

where r_1 and r_2 are the charge radii of the two nuclei. The value of δf_{nuc} is uncertain because of the uncertainties of r_1 and r_2 . The density values $\langle V_{\delta,i} \rangle_{v,N}$ decrease as the vibration becomes more excited (larger v), because the molecule becomes more stretched. For HD^+ , $\langle V_{\delta,i} \rangle_{v,N=0}$ varies from approximately 0.21 for $v = 0$ to approximately 0.17 for $v = 9$ to approximately 0.16 for $v = 18$. For the following, it is important to note that the values for proton and deuteron are close, differing only by 0.14% or less for $v \leq 9$ and by 1.5% for $v = 18$.

The following nuclear charge radius data have been recommended by CODATA 2018 [14]:

$$\begin{aligned} r_{p,2018}^2 &= 0.7080(32) \text{ fm}^2, \\ r_{d,2018}^2 &= 4.5283(31) \text{ fm}^2. \end{aligned} \quad (3)$$

The two uncertainties are almost perfectly correlated, because the deuteron-proton radius difference $r_d^2 - r_p^2$ is strongly constrained by the measurement of the isotope shift of the 1S-2S transition in H and D. Its recommended value is

$$(r_d^2 - r_p^2)_{2018} = 3.82036(41) \text{ fm}^2. \quad (4)$$

We can reexpress Eq. (2) as

$$\begin{aligned} \delta f_{\text{nuc}} &= 2cR_\infty \frac{2\pi}{3} a_0^{-2} \frac{1}{2} \left((r_1^2 + r_2^2) [\langle V_{\delta,1} \rangle_{v',N'} + \langle V_{\delta,2} \rangle_{v',N'} - (\langle V_{\delta,1} \rangle_{v,N} + \langle V_{\delta,2} \rangle_{v,N})] \right. \\ &\quad \left. + (r_1^2 - r_2^2) [\langle V_{\delta,1} \rangle_{v',N'} - \langle V_{\delta,2} \rangle_{v',N'} - (\langle V_{\delta,1} \rangle_{v,N} - \langle V_{\delta,2} \rangle_{v,N})] \right) \\ &= 2cR_\infty \frac{2\pi}{3} a_0^{-2} \frac{1}{2} \left[(r_1^2 + r_2^2) (\langle V_{\delta,12} \rangle_{v',N'} - \langle V_{\delta,12} \rangle_{v,N}) \right. \\ &\quad \left. + (r_1^2 - r_2^2) (\langle \Delta V_{\delta,12} \rangle_{v',N'} - \langle \Delta V_{\delta,12} \rangle_{v,N}) \right], \end{aligned} \quad (5)$$

with the notations $\langle V_{\delta,12} \rangle = \langle V_{\delta,1} + V_{\delta,2} \rangle$ and $\langle \Delta V_{\delta,12} \rangle = \langle V_{\delta,1} - V_{\delta,2} \rangle$.

For homonuclear MHIs the second term in square brackets is zero by definition. In order to keep the analytical model simple, for heteronuclear MHIs we ignore the nominal value

of the second term, i.e., its value for $r_i = r_{i,2018}$. For actual computations it could easily be included. We also neglect its uncertainty, which can be justified as follows. In a given fit scenario, we obtain the order of magnitude of the uncertainty of the combination $r_1^2 + r_2^2$ appearing in the first term. The uncertainty of the combination $r_1^2 - r_2^2$ will be similar or smaller for some scenarios, e.g., when both HD^+ and H_2^+ data are included. In any case, the multiplying factor $\langle \Delta V_\delta \rangle_{v',N'} - \langle \Delta V_\delta \rangle_{v,N}$ is a factor of at least 6 smaller than $\langle V_\delta \rangle_{v',N'} - \langle V_\delta \rangle_{v,N}$ (see column 7 in Table I). Thus, we may neglect the uncertainty of the second term in square brackets compared to the uncertainty of the first term. We may improve on this approximation in an extended model, where we would incorporate the experimental results from H or D spectroscopy, i.e., the result (4) together with its uncertainty, in the second term. Its uncertainty would then be negligible.

Thus, the uncertainty of δf_{nuc} is approximately

$$\begin{aligned} u(\delta f_{\text{nuc}}) &\simeq 2cR_\infty(2\pi/3)a_0^{-2} \frac{1}{2} u(r_{1,2018}^2 + r_{2,2018}^2) (\langle V_{\delta,12} \rangle_{v',N'} - \langle V_{\delta,12} \rangle_{v,N}) \\ &= 15.6 \text{ kHz} \times (\langle V_{\delta,pd} \rangle_{v',N'} - \langle V_{\delta,pd} \rangle_{v,N}) \quad (\text{HD}^+) \\ &= 15.7 \text{ kHz} \times (\langle V_{\delta,pp} \rangle_{v',N'} - \langle V_{\delta,pp} \rangle_{v,N}) \quad (\text{H}_2^+). \end{aligned} \quad (6)$$

In the second line, for HD^+ , we inserted the uncertainty $u(r_{p,2018}^2 + r_{d,2018}^2) = 0.0063 \text{ fm}^2$, where correlation has been taken into account.

We now discuss uncertainties of purely theoretical origin. They mainly concern the QED correction δf_{QED} and arise dominantly from QED contributions of high order in α ($R_\infty \alpha^6$ and above). An important point is that the largest sources of uncertainties are described by terms that are also proportional to $\langle V_{\delta,12} \rangle_{v',N'} - \langle V_{\delta,12} \rangle_{v,N}$ [6]. The largest one is the higher-order remainder of the one-loop self-energy correction, which has an estimated uncertainty

$$\begin{aligned} u(\delta f_{\text{QED},1}) &= 2cR_\infty \times 41.2\alpha^6 (\langle V_{\delta,12} \rangle_{v',N'} - \langle V_{\delta,12} \rangle_{v,N}) \\ &= 40.9 \text{ kHz} \times (\langle V_{\delta,12} \rangle_{v',N'} - \langle V_{\delta,12} \rangle_{v,N}). \end{aligned} \quad (8)$$

The second largest source of uncertainty is the higher-order remainder of the two-loop QED correction. The uncertainty

associated with this term is

$$\begin{aligned} u(\delta f_{\text{QED},2}) &= 2cR_\infty \times 90.1 \frac{\alpha^6}{\pi} (\langle V_{\delta,12} \rangle_{v',N'} - \langle V_{\delta,12} \rangle_{v,N}) \\ &= 28.5 \text{ kHz} \times (\langle V_{\delta,12} \rangle_{v',N'} - \langle V_{\delta,12} \rangle_{v,N}). \end{aligned} \quad (9)$$

A smaller uncertainty in δf_{QED} arises from the fact that some of the QED corrections at orders $R_\infty \alpha^4$ and $R_\infty \alpha^5$ have been computed in the adiabatic approximation. This is the case for the relativistic correction of order $R_\infty \alpha^4$ [20] and for the one-loop self-energy and vacuum polarization at order $R_\infty \alpha^5$ [21,22]. The corresponding uncertainties are estimated from the relative difference between the expectation values of an operator of the type $V_{\delta,12}$ calculated in the adiabatic approximation on the one hand and in an exact three-body approach on the other hand. These uncertainties are not proportional to $\langle V_{\delta,12} \rangle_{v',N'} - \langle V_{\delta,12} \rangle_{v,N}$. Moreover, they have very different dependences on the rovibrational degrees of freedom: They are small for transitions between low-lying states and increase when more excited states are involved, whereas $\langle V_{\delta,12} \rangle_{v,N}$ decreases with v and N . Due to this, the theoretical errors affecting different transitions are only imperfectly correlated. However, even for transitions between high-lying states, uncertainties associated with the adiabatic approximation remain much smaller than those from uncalculated higher-order terms [Eqs. (8) and (9)], so the theoretical uncertainties of all the transitions considered in this work are strongly correlated to each other (see Table IV). This is why in Sec. II we neglect uncertainties due to the adiabatic approximation, allowing unknown theoretical contributions to be described by a single unknown parameter. This simplified model yields analytical formulas for the uncertainties of fundamental constants as determined from HMI spectroscopy, which is very useful to guide the choice of an optimal set of transitions. The results of this model are verified by performing a least-squares adjustment (LSA) where imperfect correlations between theoretical uncertainties are taken into account (see Sec. III).

There are two other smaller sources of uncertainty from unknown QED contributions. One is a yet uncalculated part of the recoil correction of order $R_\infty \alpha^4 (m_e/m_i)$, with estimated uncertainty [20]

$$\begin{aligned} u(\delta f_{\text{QED},3}) &= 2cR_\infty \alpha^4 \frac{\pi}{16} \left((\langle V_{\delta,1} \rangle_{v',N'} - \langle V_{\delta,1} \rangle_{v,N}) \frac{m_e}{m_1} \right. \\ &\quad \left. + (\langle V_{\delta,2} \rangle_{v',N'} - \langle V_{\delta,2} \rangle_{v,N}) \frac{m_e}{m_2} \right). \end{aligned} \quad (10)$$

This can be reexpressed in terms of $\langle V_{\delta,12} \rangle$ and $\langle \Delta V_{\delta,12} \rangle$ similarly to the nuclear-size shift [Eq. (5)]. Again, the term proportional to $\langle \Delta V_{\delta,12} \rangle$ is either zero for homonuclear ions or much smaller for heteronuclear ones and may be neglected. The uncertainty then simplifies to

$$\begin{aligned} u(\delta f_{\text{QED},3}) &= 2cR_\infty \alpha^4 \frac{m_e}{\mu_{12}} \frac{\pi}{32} (\langle V_{\delta,12} \rangle_{v',N'} - \langle V_{\delta,12} \rangle_{v,N}) \\ &= 1.5 \text{ kHz} \times (\langle V_{\delta,pd} \rangle_{v',N'} - \langle V_{\delta,pd} \rangle_{v,N}) \quad (\text{HD}^+) \end{aligned} \quad (11)$$

$$= 2.0 \text{ kHz} \times (\langle V_{\delta,pp} \rangle_{v',N'} - \langle V_{\delta,pp} \rangle_{v,N}) \quad (\text{H}_2^+), \quad (12)$$

where $\mu_{12} = m_1 m_2 / (m_1 + m_2)$.

Finally, the higher-order nuclear correction $\delta f_{\text{nuc,ho}}$ [last term in Eq. (2)] is negligibly small for the proton. Only the corrections for the deuteron are included in the theoretical transition frequency, with a small associated uncertainty of [6]

$$\begin{aligned} u(\delta f_{\text{nuc,ho}}) &= 0.45 \text{ kHz} \times (\langle V_{\delta,d} \rangle_{v',N'} - \langle V_{\delta,d} \rangle_{v,N}) \\ &\simeq 0.23 \text{ kHz} \times (\langle V_{\delta,12} \rangle_{v',N'} - \langle V_{\delta,12} \rangle_{v,N}). \end{aligned} \quad (13)$$

The combined uncertainty of the contributions given in Eqs. (7)–(9), (12), and (13) is $u_0(k)(\langle V_{\delta,12} \rangle_{v',N'} - \langle V_{\delta,12} \rangle_{v,N})_k$, where $u_0(\text{HD}^+) \simeq 52.2 \text{ kHz}$ and $u_0(\text{H}_2^+) \simeq 52.3 \text{ kHz}$, which includes a 49.9-kHz contribution from purely theoretical uncertainties and a 15.6-kHz contribution due to the uncertainty of nuclear charge radii in HD^+ (15.7 kHz in H_2^+). For the vibrational transitions in Table I the purely theoretical part corresponds to a fractional frequency uncertainty of approximately 8×10^{-12} . This is a main result of the theory in Ref. [6]. Note that the value of the theoretical uncertainty has no influence on results deduced from the analytical model (see the next section) but is important for the approach based on a LSA (Sec. III).

One last point related to theoretical uncertainties is worth mentioning. Whereas all contributions to theoretical transition frequencies so far have been computed with negligibly small numerical uncertainties, this may be much harder to achieve for some of the transitions studied in this work, which involve levels with high vibrational quantum numbers such as $v = 18$ (see Tables I and II). In particular, accurate calculation of the nonrelativistic Bethe logarithm [23] for such states is a very serious numerical challenge. However, this obstacle is not of a fundamental nature, and in the present exploratory analysis we will assume that it can be overcome in the future.

II. ANALYTICAL MODEL

A. Master equation

Above we clarified that the combined uncertainty of the transition frequency arising from nuclear and QED effects is, to a good approximation, proportional to the δ -potential difference of lower and upper spectroscopy levels. This is the key point for our analytical model. We recast this uncertainty as an unknown correction to be determined from experiments. To quantify the correction, we introduce the species-dependent dimensionless parameter $\Delta_{\text{nuc,QED}}(k)$ that describes the combined deviations from the “best” theory values,

$$\begin{aligned} \Delta_{\text{nuc,QED}}(k) &(\langle V_{\delta,12} \rangle_{v',N'} - \langle V_{\delta,12} \rangle_{v,N})_k (2cR_\infty \alpha^5) \\ &= \Delta(\delta f_{\text{nuc}} + \delta f_{\text{nuc,ho}} + \delta f_{\text{QED},1} + \delta f_{\text{QED},2} + \delta f_{\text{QED},3}), \end{aligned}$$

where k denotes the molecular species. $\Delta \delta f_i$ is the unknown deviation of the actual contribution of type i from the currently calculable one.

According to the discussion above, the recoil correction $\delta f_{\text{QED},3}$ is species dependent. There are different possibilities for its treatment. The correction is amenable to an *ab initio* calculation [24], and this calculation is expected to be easier than reducing $u(\delta f_{\text{QED},1})$ or $u(\delta f_{\text{QED},2})$. In this case, we would be allowed to ignore the correction in the present context. Alternatively, we could incorporate the recoil correction into

TABLE II. Some rovibrational transitions of H_2^+ and their properties. The first transition has recently been observed [16]. Transitions 2 and 3 have substantial positive sensitivity s . Transition 4 has a suppressed sensitivity. In this table, $V_\delta \equiv V_{\delta,pp}$.

No.	Transition (v, N) \rightarrow (v', N')	Frequency f (THz)	$f_{\text{nr,a.u.}}$	s $\partial f_{\text{nr,a.u.}}/\partial(m_p/m_e)$	V $\langle V_\delta \rangle_{v',N'} - \langle V_\delta \rangle_{v,N}$
1	(1, 0) \rightarrow (3, 2)	124	0.0189	-4.531×10^{-6}	-0.02049
2	(11, 0) \rightarrow (13, 2)	53.4	0.00811	1.516×10^{-6}	-0.007464
3	(12, 0) \rightarrow (14, 2)	45.9	0.00698	2.284×10^{-6}	-0.006314
4	(9, 0) \rightarrow (11, 2)	67.7	0.0103	1.572×10^{-7}	-0.009773

$\Delta_{\text{nuc}}(k)$. With any of these treatments, we may write

$$\Delta_{\text{nuc,QED}}(k) = \Delta_{\text{nuc}}(k) + \Delta_{\text{nuc,ho}}(k) + \Delta_{\text{QED}},$$

where all quantities are dimensionless and independent of the levels and Δ_{QED} is also independent of the molecule species.

The Rydberg constant is also affected by uncertainty. We introduce the fractional deviation with respect to the CODATA 2018 value $\Delta_h = R_\infty/R_{\infty,2018} - 1$.

In summary, we may express a theoretical spin-averaged frequency as

$$\begin{aligned} & f^{(\text{theor})}(v, N, v', N') \\ &= f_{2018}^{(\text{theor})}(v, N, v', N') + 2cR_{\infty,2018} \left(\Delta_h f_{2018,\text{a.u.}}^{(\text{theor})}(v, N, v', N') \right. \\ & \quad \left. + \sum_{i=1,2} \Delta_{m,i} \partial f_{2018,\text{a.u.}}^{(\text{theor})}(v, N, v', N') / \partial(m_i/m_e) \right. \\ & \quad \left. + \Delta_{\text{nuc,QED}} \alpha^5 (\langle V_\delta \rangle_{v',N'} - \langle V_\delta \rangle_{v,N}) \right), \end{aligned} \quad (14)$$

where $\Delta_{m,i} = m_i/m_e - (m_i/m_e)_{2018}$ and the molecule-species dependence k is implicit. Here $f_{2018}^{(\text{theor})}(v, N, v', N')$ is the *ab initio* transition frequency computed with the CODATA 2018 fundamental constants and no uncertainty is associated with it. A subscript a.u. indicates that the frequency is expressed in atomic units. The above master equation is a generalization of Eq. (16) of Ref. [20]. (While the master equation has been stated with CODATA 2018 values, these are just reference values; the equation would be just as applicable if we used CODATA 2014 reference values instead.) There is one such master equation for each MHI species. For homonuclear MHIs, appropriate simplifications hold. Considering all six MHI species (enumerated by the index k), there are ten unknown parameters $\Delta_{m,p}$, $\Delta_{m,d}$, $\Delta_{m,t}$, $\{\Delta_{\text{nuc,QED}}(k)\}$, and Δ_h .

The master equation is approximate, since we have explicitly neglected some terms that arise for heteronuclear MHIs and because additional small uncertainties are present in the theoretical transition frequency that stem from the use of adiabatic wave function to calculate several QED contributions and do not have the simple form of the last term in Eq. (14). For exploratory analyses such as the present one, in the second and third lines of Eq. (14), $f_{2018}^{(\text{theor})}$ may be replaced by f_{nr} , the theoretical nonrelativistic frequency. The latter can be approximated by the adiabatic transition frequency, obtained by solving the one-dimensional radial Schrödinger equation with the adiabatic potential [25] appropriate to each species.

For heteronuclear MHIs, the two mass-deviation contributions from m_1 and m_2 may be approximately subsumed into a single one concerning the reduced nuclear mass μ_{12} ,

$$\Delta_{m,\lambda} \frac{\partial f_{\text{nr,a.u.}}(v, N, v', N')}{\partial \lambda},$$

with $\lambda = \mu_{12}/m_e$ and $\Delta_{m,\lambda} = \mu_{12}/m_e - (\mu_{12}/m_e)_{2018}$. This approximation is good, because the nonrelativistic transition frequency is well approximated by the difference of the adiabatic energies.

For reference, the current (CODATA 2018) uncertainties of the mass-ratio deviations are $u(\Delta_{m,p,2018}) = 1.1 \times 10^{-7}$, $u(\Delta_{m,d,2018}) = 1.3 \times 10^{-7}$, and $u(\Delta_{m,t,2018}) = 2.7 \times 10^{-7}$. Furthermore, the (current) uncertainty of $\Delta_{\text{nuc,QED}}$ is $u(\Delta_{\text{nuc,QED}}(\text{HD}^+)) \simeq 52 \text{ kHz}/2cR_\infty\alpha^5 \simeq 0.38$, and similar for H_2^+ . The uncertainty of $\lambda = \mu_{pd}/m_e$ is $u([\Delta_{m,\lambda}(\text{HD}^+)]_{2018}) = 5.6 \times 10^{-8}$, or 4.6×10^{-11} in relative terms. The uncertainty of this last quantity deduced from recent Penning trap experiments [8–11] is moderately smaller [7] (see Fig. 1). All of these uncertainties do not enter the present treatment.

The Rydberg constant fractional uncertainty is $u(\Delta_{h,2018}) = 1.9 \times 10^{-12}$. This is a relevant quantity only in the simplest scenario outlined here, the measurement of a transition pair (see Table I in the Supplemental Material [26]).

B. Transitions

Table I presents the relevant parameters for a number of electric dipole allowed transitions of HD^+ . A few electric quadrupole transitions of H_2^+ having $v' - v = 2$ are reported in Table II.

The mass sensitivities, denoted by s or β_λ in the following sections, as well as the expectation values of the δ functions, $\langle V_\delta \rangle$, are obtained from nonadiabatic (exact) nonrelativistic calculations, a choice which may be relevant especially for transitions involving large vibrational quantum numbers. To compute the mass sensitivities, we follow an approach similar to that of Ref. [17]. The Hamiltonian [Eq. (6) of [17]] is reexpressed as a function of the variables μ_{pd}/m_e and m_p/m_e and then the derivatives are easily found to be equal to some combinations of the kinetic energy operator expectation values. Their expressions can be found in Eqs. (13b) and (13c) of Ref. [7].

Among the shown transitions of HD^+ are those that have already been studied experimentally to date, all having $v = 0$ as the lower level. In addition, a few hot-band transitions are included. Transition number 5 (red in Fig. 1) occurs between highly excited vibrational levels: $v = 9$ and $v' = 18$. It

exhibits the opposite sign of the sensitivity s of the frequency to the mass ratio compared to transitions having the ground vibrational level as the lower level. Transition 5 is just one of several such transitions. Also, we point out the existence of transitions that have strongly suppressed sensitivity to the mass ratio. Number 6 is an example that is shown in blue in Fig. 1. Such transitions are obviously not effective in determining the mass ratio. However, they are effective in determining the QED contribution parameter $\Delta_{\text{nuc,QED}}$ and therefore, when part of a set of transitions, contribute to determining the mass ratio. An important aspect is that while s does not scale with the transition frequency value, V is approximately proportional to it. This correlation has an important consequence: $\Delta_{\text{nuc,QED}}$ cannot be determined as accurately as the mass ratio.

C. Determination of the mass ratios and Rydberg constant

If a large enough set of experimental transition frequencies is available, a LSA of the quantities $\Delta_{m,\mu}$, $\Delta_{\text{nuc,QED}}(k)$, and Δ_h can be made using the master equation (14). Instead, for the sake of simplicity, we consider the cases of minimal-size data sets being available, so these quantities are obtained by solving a linear system of equations.

The proposed measurement approach presented here is applicable not only to HD^+ but also to all other MHI species, whose vibrational transitions have not yet been determined with laser spectroscopy with competitive accuracy. We have analyzed several scenarios. Some of them are presented in [26]. One is described in the following.

In view of the approximations made, projected uncertainty levels obtained with the analytical approach should be considered as indicative only. The analytical approach is nevertheless very useful as it allows us to identify easily the most promising transitions, as confirmed by comparison with a LSA in Sec. III.

Two species

One scenario we consider comprises three transitions in HD^+ and two transitions in H_2^+ . This will allow us to determine the five quantities μ_{pd}/m_e , m_p/m_e , $\Delta_{\text{nuc,QED}}(\text{H}_2^+)$, $\Delta_{\text{nuc,QED}}(\text{HD}^+)$, and R_∞ that appear in the two corresponding master equations. Once μ_{pd}/m_e and m_p/m_e have been obtained, the deuteron mass m_d/m_e becomes available. Data from more than five transitions would be very useful for consistency checks and would then be analyzed using LSA.

Let us first consider a general aspect of this scenario. Recall the deviations $\Delta_{\text{nuc,QED}}(\text{H}_2^+)$ and $\Delta_{\text{nuc,QED}}(\text{HD}^+)$ in terms of their contributions, the charge radii deviations, the QED deviation, and the higher-order nuclear deviation (if present),

$$\Delta_{\text{nuc,QED}}(\text{H}_2^+) = \alpha^{-5}(2\pi/3)a_0^{-2}\frac{1}{2} \times 2\Delta(r_p^2) + \Delta_{\text{QED}}, \quad (15)$$

$$\begin{aligned} \Delta_{\text{nuc,QED}}(\text{HD}^+) &= \alpha^{-5}(2\pi/3)a_0^{-2}\frac{1}{2}\Delta(r_p^2 + r_d^2) \\ &+ \Delta_{\text{QED}} + \Delta_{\text{nuc,ho}}(d). \end{aligned} \quad (16)$$

Small corrections have been neglected. Note that Δ_{QED} is independent of the molecular species, under the assumptions made. We may compare the contributions on each right-hand side, in other words, their uncertainties. The

uncertainty of the first contribution is of order 0.11. The uncertainty of the second, $u(\Delta_{\text{QED}})$, is of order $50\alpha \approx 0.37$, according to Eqs. (8) and (9). Finally, $u(\Delta_{\text{nuc,ho}}(d)) \simeq (0.23 \text{ kHz})/2cR_\infty\alpha^5 = 0.0017$ [Eq. (13)]. Once fit results for $\Delta_{\text{nuc,QED}}(\text{H}_2^+)$ and $\Delta_{\text{nuc,QED}}(\text{HD}^+)$ are obtained, we can obtain from Eqs. (15) and (16) an approximate value for the difference of the squared radii of the deuteron and proton,

$$\begin{aligned} \Delta(r_d^2) - \Delta(r_p^2) &\simeq 2(2\pi/3)^{-1}a_0^2\alpha^5[\Delta_{\text{nuc,QED}}(\text{HD}^+) \\ &- \Delta_{\text{nuc,QED}}(\text{H}_2^+) - \Delta_{\text{nuc,ho}}(d)]. \end{aligned} \quad (17)$$

The mentioned uncertainty of the last term sets the minimum possible uncertainty of the left-hand side, $9 \times 10^{-5} \text{ fm}^2$. This is a factor 4.5 less than the CODATA 2018 uncertainty [Eq. (4)].

Table III shows the result of a particular measurement scenario: three HD^+ transitions found to be favorable (see [26]) and two transitions in H_2^+ . For frequency uncertainties at the 1-Hz level (last line in the table), the uncertainty of the Rydberg constant is one order smaller than CODATA 2018, while for μ_{pd}/m_e it is two orders and for m_p/m_e it is three orders smaller. The uncertainty of $\Delta_{\text{nuc,QED}}(\text{HD}^+) - \Delta_{\text{nuc,QED}}(\text{H}_2^+)$ is smaller than that of $\Delta_{\text{nuc,ho}}(d)$ (see the rightmost column in the table). This implies an experimental uncertainty for $\Delta(r_d^2) - \Delta(r_p^2)$ four times smaller than the CODATA 2018 uncertainty. These results are encouraging and will be verified in the next section using a more rigorous approach.

III. SIMULATIONS OF FUNDAMENTAL CONSTANT DETERMINATIONS USING LEAST-SQUARES ADJUSTMENTS

The analysis presented in Sec. II relies on the assumption that the combined uncertainty of a transition frequency arising from nuclear and QED effects can be described by a single term proportional to the δ -potential difference between the lower and upper levels. As already noted, this is only approximately true, because one of the contributions to the theoretical uncertainty cannot be written under this form, namely, the uncertainty arising from the use of the adiabatic approximation in the calculation of high-order QED corrections. A more elaborate description that takes into account the imperfect correlations between theoretical uncertainties of different rovibrational transition frequencies is thus required to verify the insights given by our simple analytical model and obtain more precise estimates of achievable precision of fundamental constant determinations from MHI spectroscopy. In the following, we use the linearized least-squares adjustment procedure described in Appendix E of [13]. See also [7] for a recent application to MHI spectroscopic data.

Each of the (hypothetical) transition frequency measurements yields the following observational equations:

$$\begin{aligned} f^{(\text{expt})} &\doteq f^{(\text{theor})} + \delta f^{(\text{theor})} + \beta_\lambda(\lambda - \lambda_0) + \beta_{R_\infty}c(R_\infty - R_{\infty 0}) \\ &+ \beta_{r_i}(r_i - r_{i0}), \end{aligned} \quad (18)$$

$$\delta f \doteq \delta f^{(\text{theor})}. \quad (19)$$

The dotted equality sign means that the left- and right-hand sides should agree within estimated uncertainties. In addition, $f^{(\text{expt})}$ and $f^{(\text{theor})}$ are the experimental and theoretical tran-

TABLE III. Analytical model: determination of the five quantities m_p/m_e , $\lambda = \mu_{pd}/m_e$, Rydberg constant, and nuclear QED corrections $\Delta_{\text{nuc,QED}}(\text{H}_2^+)$ and $\Delta_{\text{nuc,QED}}(\text{HD}^+)$ by measuring five transitions, three in HD^+ and two in H_2^+ . Columns 1–3 indicate the chosen transitions of HD^+ (a–c); columns 4 and 5 refer to the transitions of H_2^+ (d and e). The transition labels are defined in previous tables. Column 6 lists the assumed experimental uncertainties. The other columns give the absolute uncertainties of the determined quantities. Note that the fractional uncertainty of the Rydberg constant $u_r(R_\infty)$ is equal to $u(\Delta_n)$. We used the abbreviations $\Delta_{\text{HD}^+} = \Delta_{\text{nuc,QED}}(\text{HD}^+)$ and $\Delta_{\text{H}_2^+} = \Delta_{\text{nuc,QED}}(\text{H}_2^+)$.

Transitions					u_a, u_b, u_c, u_d, u_e	$u(\Delta_{m,\lambda})$	$u(\Delta_{m,p})$	$u_r(R_\infty)$	$u(\Delta_{\text{HD}^+})$	$u(\Delta_{\text{H}_2^+})$	$u(\Delta_{\text{HD}^+} - \Delta_{\text{H}_2^+})$
a	b	c	d	e	(kHz)	(10^{-10})	(10^{-10})	(10^{-12})			
3	4	5	1	2	0.3, 0.3, 0.3, 0.3, 0.1	130	220	55	2.7	2.7	0.11
3	4	5	1	2	0.1, 0.1, 0.1, 0.1, 0.03	44	74	18	0.91	0.89	0.037
3	4	5	1	2	0.03, 0.03, 0.03, 0.03, 0.03	13	26	5.5	0.27	0.27	0.018
3	4	5	1	2	0.003, 0.003, 0.003, 0.01, 0.01	1.3	5.5	0.55	0.027	0.027	0.0055
3	4	5	1	2	0.003, 0.003, 0.003, 0.003, 0.003	1.3	2.6	0.55	0.027	0.027	0.0018
3	4	5	1	2	0.003, 0.003, 0.003, 0.001, 0.001	1.3	2.2	0.55	0.027	0.027	0.0010
3	4	5	1	2	0.001, 0.001, 0.001, 0.001, 0.001	0.44	0.87	0.18	0.0091	0.0089	0.00061

sition frequencies, respectively. The latter is obtained using reference, e.g., CODATA 2018, values of the involved fundamental constants: the mass ratio λ , the Rydberg constant, and the nuclear charge radii r_i . The dependence of the theoretical frequency on these constants is linearized around their reference values λ_0 , $R_{\infty 0}$, and r_{i0} using the sensitivity coefficients $\beta_\lambda = \partial f^{(\text{theor})}/\partial \lambda \simeq \partial f_{\text{nr}}^{(\text{theor})}/\partial \lambda$, $\beta_{R_\infty} = f^{(\text{theor})}/cR_\infty$, and $\beta_{r_i} = \partial f^{(\text{theor})}/\partial r_i$. For heteronuclear molecules, Eq. (18) contains an implicit summation over i , and $\lambda \equiv \mu_{12}/m_e$, with μ_{12} the reduced mass of the nuclei. For homonuclear molecules, $\lambda \equiv m_i/m_e$, with m_i the mass of a nucleus.

The theoretical uncertainty of the transition frequency is accounted for by introducing the additive correction $\delta f^{(\text{theor})}$, which is treated as an adjusted constant. A second input datum with zero value ($\delta f \equiv 0$) and uncertainty equal to the estimated theoretical uncertainty is included in the LSA [Eq. (19)].

We take into account correlations between different input data. Measurements of different transitions are assumed to be uncorrelated to each other, but theoretical uncertainties are strongly correlated. The correlation coefficients among the δf are estimated using the results of [6] and can be found in Table IV.

A. Two transitions in one species

We first consider the scenario where two transitions are measured in HD^+ . Since in this case we are only aiming to determine the mass ratio μ_{pd}/m_e , additional data are required on the other involved fundamental constants R_∞ , r_p , and r_d . We thus include the following observational equations:

$$R_{\infty,2018} \doteq R_\infty, \quad (20)$$

$$r_{i,2018} \doteq r_i \quad (i = p, d). \quad (21)$$

The correlation coefficients between the CODATA 2018 values of these constants are $r(R_{\infty,2018}, r_{p,2018}) = 0.885\,92$, $r(R_{\infty,2018}, r_{d,2018}) = 0.903\,66$, and $r(r_{p,2018}, r_{d,2018}) = 0.991\,65$. The total number of input data is $N = 7$ (two experimental frequencies, two associated δf , and the three CODATA 2018 values), whereas the number of adjusted constants is $M = 6$ (μ_{pd}/m_e , R_∞ , r_p , r_d , and the two $\delta f^{(\text{theor})}$). Results are displayed in the last column of Table I in [26].

As already indicated by the analytical model (see the Supplemental Material [26]), we recognize the importance of the choice of transition pair: (3,5) is substantially more favorable than (3,4). The lowest LSA uncertainty among the examples is approximately 3×10^{-9} , a factor 8 lower than what is obtained from two of the currently available measurements (last row in the table) and a factor 19 smaller than the CODATA 2018 uncertainty.

In the case of H_2^+ , two measurements may already offer the possibility to determine other constants in addition to m_p/m_e . However, two transitions are still not sufficient to determine the three constants involved, m_p/m_e , R_∞ , and r_p , and some additional input data is required. It would make little sense to include the CODATA 2018 value of, e.g., r_p in order to determine m_p/m_e and R_∞ because the proton charge radius is strongly correlated to the Rydberg constant by the very precise measurements of the 1S-2S transition frequency in the H atom [27,28]. We instead include these 1S-2S measurements and associated theoretical δf correction [similarly to Eq. (19)] in our LSA using the information provided in [14] (items A6 and A7 from Table X, B1 and B2 from Table VIII, and their correlation coefficients from Table IX therein). The uncertainty of the theoretical correction is 1.4 kHz. The total number of input data is $N = 7$ [two H_2^+ experimental frequencies, two associated δf , the two H(1S-2S) measurements, and one associated δf], whereas the number of adjusted constants is $M = 6$ [m_p/m_e , R_∞ , r_p , the two $\delta f^{(\text{theor})}(\text{H}_2^+)$, and one $\delta f^{(\text{theor})}(\text{H})$].

Results are displayed in Table V. We see that there is no further gain in pursuing an experimental frequency uncertainty smaller than 0.1 kHz. For that case, the mass-ratio uncertainty, of order approximately 4.7×10^{-12} fractionally, is 13 times smaller than the CODATA 2018 uncertainty.

B. Three transitions in one species

Similarly, three transition measurements in HD^+ could be used to determine the Rydberg constant and nuclear radii r_p and r_d . To do this, we again include the H(1S-2S) measurements [27,28], but also the H-D(1S-2S) isotope shift measurement [29] (item A5 from Table X, B17 and B18 from Table VIII, and correlation coefficients from Table IX therein). The theory uncertainty is set to 0.34 kHz. The total

TABLE IV. Correlation coefficients between theoretical uncertainties of HD^+ and H_2^+ transition frequencies. The arguments are the transition numbers, defined in Tables I and II.

Correlation coefficients				
Among HD^+ transitions				
$r(1, 2) = 0.99570$	$r(1, 3) = 0.98071$	$r(1, 4) = 0.95733$	$r(1, 5) = 0.91011$	$r(1, 6) = 0.86385$
$r(1, 7) = 0.84570$	$r(1, 8) = 0.87967$	$r(2, 3) = 0.99460$	$r(2, 4) = 0.97998$	$r(2, 5) = 0.94457$
$r(2, 6) = 0.90678$	$r(2, 7) = 0.89148$	$r(2, 8) = 0.91993$	$r(3, 4) = 0.99535$	$r(3, 5) = 0.97355$
$r(3, 6) = 0.94565$	$r(3, 7) = 0.93370$	$r(3, 8) = 0.95566$	$r(4, 5) = 0.99102$	$r(4, 6) = 0.97257$
$r(4, 7) = 0.96383$	$r(4, 8) = 0.97958$	$r(5, 6) = 0.99493$	$r(5, 7) = 0.99081$	$r(5, 8) = 0.99766$
$r(6, 7) = 0.99939$	$r(6, 8) = 0.99948$	$r(7, 8) = 0.99774$		
Among H_2^+ transitions				
$r(1, 2) = 0.93922$	$r(1, 3) = 0.93365$	$r(1, 4) = 0.92866$	$r(2, 3) = 0.99987$	$r(2, 4) = 0.99956$
$r(3, 4) = 0.99991$				
Between HD^+ and H_2^+ transitions				
$r(1, 1) = 0.99083$	$r(1, 2) = 0.88436$	$r(1, 3) = 0.87684$	$r(1, 4) = 0.87018$	$r(2, 1) = 0.99904$
$r(2, 2) = 0.92377$	$r(2, 3) = 0.91758$	$r(2, 4) = 0.91206$	$r(3, 1) = 0.99804$	$r(3, 2) = 0.95852$
$r(3, 3) = 0.95388$	$r(3, 4) = 0.94969$	$r(4, 1) = 0.98748$	$r(4, 2) = 0.98149$	$r(4, 3) = 0.97833$
$r(4, 4) = 0.97541$	$r(5, 1) = 0.95759$	$r(5, 2) = 0.99826$	$r(5, 3) = 0.99721$	$r(5, 4) = 0.99610$
$r(6, 1) = 0.92378$	$r(6, 2) = 0.99905$	$r(6, 3) = 0.99960$	$r(6, 4) = 0.99987$	$r(7, 1) = 0.90982$
$r(7, 2) = 0.99696$	$r(7, 3) = 0.99806$	$r(7, 4) = 0.99881$	$r(8, 1) = 0.93566$	$r(8, 2) = 0.99990$
$r(8, 3) = 0.99993$	$r(8, 4) = 0.99976$			

number of input data is $N = 11$ (three HD^+ experimental frequencies, three associated δf , the three H-D(1S-2S) measurements, and two associated δf), whereas the number of adjusted constants is $M = 9$ [μ_{pd}/m_e , R_∞ , r_p , r_d , the three $\delta f^{(\text{theor})}(\text{HD}^+)$, $\delta f^{(\text{theor})}(\text{H})$, and $\delta f^{(\text{theor})}(\text{H-D})$].

Results are displayed in Table VI. The first case in the table (data row 1) considers the three rovibrational transitions measured to date. In this case, the uncertainty of the fitted mass ratio μ_{pd} is not competitive because no input values of the Rydberg constant and nuclear radii are provided. Among the examples, the lowest LSA uncertainty for the mass ratio is approximately 3×10^{-9} , the same value as for the case of two transitions only. Now, also the charge radii are determined, but their uncertainties are approximately one order larger than from muonic hydrogen and deuterium measurements.

TABLE V. Linearized LSA procedure. Listed are examples of determination of m_p/m_e , Rydberg constant, and proton charge radius by measuring two transitions a and b in H_2^+ . The H(1S-2S) measurements are included in the input data. Here u_r denotes a fractional uncertainty and u an absolute uncertainty.

Transitions		u_a, u_b	$u_r(m_p/m_e)$	$u_r(R_\infty)$	$u(r_p)$
a	b	(kHz)	(10^{-12})	(10^{-12})	(fm)
1	3	0.3, 0.3	7.4	27	0.029
1	3	0.1, 0.1	4.7	25	0.027
1	3	0.03, 0.03	4.3	25	0.027
1	3	0.01, 0.01	4.2	25	0.027
1	3	0.003, 0.003	4.2	25	0.027
1	3	0.001, 0.001	4.2	25	0.027
CODATA 2018			60	1.9	0.0019

C. Two species

Here we consider the case where three transition measurements in HD^+ and two in H_2^+ are available. In principle, this is enough to determine the five quantities μ_{pd}/m_e , m_p/m_e , Rydberg constant, and proton and deuteron charge radii. The LSA then comprises $N = 10$ input data (the five experimental frequencies and five associated δf) and $M = 10$ adjusted constants (μ_{pd}/m_e , m_p/m_e , R_∞ , r_p , r_d , and the five $\delta f^{(\text{theor})}$).

Results are displayed in Table VII. We see that the uncertainties “saturate” once the experimental frequency uncertainties are at the 10-Hz level. There is no substantial reduction of the uncertainty of the reduced proton-deuteron mass ratio compared to the case of only three HD^+ transitions; however, a strong (sixfold) reduction in the uncertainty of the proton-electron mass ratio compared to the case of only two H_2^+ transitions is obtained. The uncertainty of the deuteron charge radius is now similar to the CODATA 2018 value. We may compare Table VII with the corresponding Table III of the analytical model. The latter overestimates the projected reduction of uncertainties by a few orders, for the smallest assumed experimental uncertainties. This is due to the assumption of perfect correlations.

Alternatively, the HD^+ data can be combined with the H(1S-2S) and H-D(1S-2S) measurements to get more accurate determinations. In this case, the number of input data is $N = 15$ (adding the three H and D experimental frequencies and two associated δf with respect to the previous adjustment), whereas the number of adjusted constants is $M = 12$ (adding the two H and D $\delta f^{(\text{theor})}$).

Results are displayed in Table VIII. When the experimental uncertainties are assumed to be 1 Hz (data row 9 in the table), i.e., fractionally 2×10^{-14} to 2×10^{-15} , depending on the transition, the uncertainties plunge by impressive factors compared to CODATA 2018: $u(\mu_{pd}/m_e)$ by a factor 600,

TABLE VI. Examples of LSA of the four constants $\lambda_{pd} = \mu_{pd}/m_e$, R_∞ , r_p , and r_d by measuring three transitions a, b, c in HD^+ . The H(1S-2S) and H-D(1S-2S) isotope shift measurements are included in the input data.

Transitions			u_a, u_b, u_c	$u_r(\lambda_{pd})$	$u_r(R_\infty)$	$u(r_p)$	$u(r_d)$
a	b	c	(kHz)	(10^{-12})	(10^{-12})	(fm)	(fm)
2	3	4	0.15, 0.6, 0.46	106	111	0.12	0.047
3	4	5	0.3, 0.3, 0.3	5.4	23	0.024	0.0095
3	4	5	0.03, 0.03, 0.03	2.2	17	0.018	0.0071
3	4	5	0.01, 0.01, 0.01	2.1	17	0.018	0.0070
3	4	5	0.003, 0.003, 0.003	2.1	17	0.018	0.0070
3	4	5	0.001, 0.001, 0.001	2.0	17	0.018	0.0070
3	5	6	0.003, 0.003, 0.003	3.0	19	0.021	0.0082
3	5	8	0.003, 0.003, 0.003	2.9	19	0.020	0.0081
3	6	7	0.003, 0.003, 0.003	2.4	18	0.019	0.0076
3	6	8	0.003, 0.003, 0.003	2.6	19	0.020	0.0078
CODATA 2018				46	1.9	0.0019	0.00074

$u(m_p/m_e)$ by a factor 1000, $u(R_\infty)$ by a factor 3.5, $u(r_p)$ by a factor 11, and $u(r_d)$ by a factor 14.

Compared to two scenarios discussed earlier, (i), (iii) in Ref. [12], the reduction of the uncertainties $u(m_p/m_e)$, $u(\mu_{pd}/m_e)$, $u(R_\infty)$, $u(r_p)$, and $u(r_d)$ is by factors 72, 110, 6, 37, and 140, respectively, where now experimental uncertainties are assumed to be two orders smaller, a different set of MHI transitions, and inclusion of different hydrogen data are considered.

It should be noted that already for experimental uncertainties on the order of $(2-5) \times 10^{-13}$, one order lower than today (data row 4 in the table), the uncertainties of the charge radii and of the Rydberg constant would be a factor 2 smaller than CODATA 2018 uncertainties and the mass-ratio uncertainties a factor of approximately 25 smaller.

Finally, Table VIII also considers, in the last two data rows, a possible substantial reduction in QED theory uncertainty. This would mainly reduce the uncertainty of r_d .

D. Transitions with weak sensitivity to the mass ratios

Related to the fact that in any species there are transitions with positive and with negative sensitivity to the relevant mass ratios, there are also transitions with small, in a few cases

very small, sensitivity. In H_2^+ , transition 4 has sensitivity 29 times smaller than for transition 1. The latter may be viewed as a reference transition, exhibiting quasiharmonic sensitivity, since its initial and final levels have small vibrational quantum numbers. Another transition $(6, 0) \rightarrow (13, 2)$ has sensitivity -6.504×10^{-9} a.u., approximately 1×10^3 times smaller. In HD^+ , transition 6 has sensitivity approximately 110 times smaller than reference transition 2, according to the nonadiabatic calculation.

The existence of such transitions opens up an additional opportunity: determination of only the set of constants (R_∞, r_p, r_d) , ignoring the mass ratios. In other words, the mass ratios are not adjusted in the LSA. Keeping the present analysis simple, we may omit the CODATA 2018 values as input to the LSA, claiming that the current uncertainties of these constants are small enough that their significance in the results of the LSA would turn out to be small. This is certainly the case, if the most appropriate transitions are chosen. CODATA 2018 values of the mass ratios are still used to compute the theoretical transition frequencies that are input to the LSA.

We show in Table IX a LSA example. In comparison with the result of Table VII that relied on five transitions, here the obtained Rydberg constant uncertainty is similar, while the radii's uncertainties are less than a factor 2 larger. All three

TABLE VII. LSA determination of the five quantities $\lambda_{pd} = \mu_{pd}/m_e$, m_p/m_e , Rydberg constant, and proton and deuteron charge radii, by measuring five transitions, three in HD^+ (a, b, c) and two in H_2^+ (d and e). No other input data are included. Columns 1–3 indicate the chosen transitions of HD^+ ; columns 4 and 5 refer to H_2^+ . The transition labels are defined in previous tables. Column 6 gives the assumed uncertainties of the measured frequencies. Fractional or absolute uncertainties of the five adjusted constants are shown in columns 7–11.

Transitions					u_a, u_b, u_c, u_d, u_e	$u_r(\lambda_{pd})$	$u_r(m_p/m_e)$	$u_r(R_\infty)$	$u(r_p)$	$u(r_d)$
a	b	c	d	e	(kHz)	(10^{-12})	(10^{-12})	(10^{-12})	(fm)	(fm)
3	4	5	1	2	0.3, 0.3, 0.3, 0.3, 0.1	3.8	8.9	43	0.068	0.0019
3	4	5	1	2	0.1, 0.1, 0.1, 0.1, 0.03	2.8	3.0	23	0.036	0.00099
3	4	5	1	2	0.03, 0.03, 0.03, 0.03, 0.03	2.7	1.3	19	0.030	0.00085
3	4	5	1	2	0.03, 0.03, 0.03, 0.01, 0.01	2.7	1.1	19	0.030	0.00082
3	4	5	1	2	0.003, 0.003, 0.003, 0.003, 0.003	2.7	0.68	19	0.030	0.00080
3	4	5	1	2	0.003, 0.003, 0.003, 0.001, 0.001	2.7	0.67	19	0.030	0.00080
3	4	5	1	2	0.001, 0.001, 0.001, 0.001, 0.001	2.7	0.67	19	0.030	0.00080
CODATA 2018						46	60	1.9	0.0019	0.00074

TABLE VIII. LSA: similar to Table VII, but with H(1S-2S) and H-D(1S-2S) measurements included as input data. The last two scenarios are computed for QED theory uncertainties 1×10^{-12} , a factor 8 smaller than elsewhere in this work. The main effect is a reduction of the uncertainty of r_d .

Transitions					u_a, u_b, u_c, u_d, u_e	$u_r(\lambda_{pd})$	$u_r(\lambda_p)$	$u_r(R_\infty)$	$u(r_p)$	$u(r_d)$
a	b	c	d	e	(kHz)	(10^{-12})	(10^{-12})	(10^{-12})	(fm)	(fm)
2	3	4	1	2	0.3, 0.3, 0.3, 0.3, 0.1	29	6.4	15	0.016	0.0062
2	3	4	1	2	0.003, 0.003, 0.003, 0.003, 0.003	2.7	0.73	1.4	0.0014	0.00053
3	4	5	1	2	0.3, 0.3, 0.3, 0.3, 0.1	3.1	5.1	2.7	0.0029	0.0011
3	4	5	1	2	0.1, 0.1, 0.1, 0.1, 0.03	1.4	2.4	1.0	0.00096	0.00037
3	4	5	1	2	0.03, 0.03, 0.03, 0.03, 0.03	0.47	1.1	0.78	0.00060	0.00023
3	4	5	1	2	0.03, 0.03, 0.03, 0.01, 0.01	0.47	0.76	0.61	0.00031	0.00011
3	4	5	1	2	0.003, 0.003, 0.003, 0.003, 0.003	0.088	0.12	0.57	0.00019	0.000055
3	4	5	1	2	0.003, 0.003, 0.003, 0.001, 0.001	0.088	0.089	0.56	0.00019	0.000051
3	4	5	1	2	0.001, 0.001, 0.001, 0.001, 0.001	0.076	0.057	0.56	0.00019	0.000051
3	4	5	1	2	0.003, 0.003, 0.003, 0.003, 0.003	0.080	0.11	0.48	0.00015	0.000025
3	4	5	1	2	0.001, 0.001, 0.001, 0.001, 0.001	0.066	0.052	0.48	0.00014	0.000013
CODATA 2018						46	60	1.9	0.0019	0.00074

uncertainties are substantially smaller than those of CODATA 2018.

For the selected H_2^+ transition 4 the impact of the CODATA 2018 uncertainty of m_p/m_e is $u_r(f_d) = 2.7 \times 10^{-13}$ and thus is twice smaller than the fractional uncertainty of the adjusted Rydberg constant in the third scenario of the table. The above assumption is thus still acceptable. If necessary, one may select a H_2^+ transition with weaker sensitivity.

E. Ratios of frequencies

When we consider different transitions in the same species or in different species, we find pairs that have similar sensitivity to the respective mass ratios. Furthermore, all transition frequencies are proportional to the Rydberg constant. Finally, the QED uncertainties are correlated. Then we may construct ratios of frequencies in which these constants or contributions are fully or partially suppressed. Frequency ratios are conceptually simple and therefore they are attractive for illustration purposes. In Ref. [5] ratios of (experimentally available) HD^+

frequencies were considered. Because appropriate ratios suppress the influence of QED uncertainties, it was argued that they can be used as figures of merit for a test of quantum mechanics.

Here we consider ratios of HD^+ and H_2^+ frequencies. By proper choice of the transition pair, such a ratio may remove the sensitivity to m_p/m_e . Indeed, this sensitivity is present also in HD^+ , where it is intertwined with the sensitivity to m_d/m_p . However, this latter ratio has been very precisely measured [11] and its uncertainty is therefore of less concern.

By inspection, we found the HD^+ transitions 11, i.e., $(v = 0, L = 0) \rightarrow (4, 1)$, and 12, i.e., $(v = 1, L = 0) \rightarrow (3, 1)$, to have fractional sensitivities $\hat{s}_{m_p/m_e} = (f_{\text{nr}})^{-1} \partial f_{\text{nr}} / \partial (m_p/m_e)$ very similar to that of reference transition 1 in H_2^+ ($\hat{s}_{m_p/m_e} = -2.3948 \times 10^{-4}$). The HD^+ sensitivities are $\hat{s}_{m_p/m_e} = (-2.3791, -2.3907) \times 10^{-4}$, respectively. The first HD^+ transition is particularly easily accessible and has already been utilized [30].

The analysis of the fractional deviation of the HD^+ (11) to H_2^+ (1) frequency ratio

$$\frac{[f_{11}(\text{HD}^+)/f_1(\text{H}_2^+)]_{(\text{theor})}}{[f_{11}(\text{HD}^+)/f_1(\text{H}_2^+)]_{(\text{expt})}} - 1 \quad (22)$$

shows that the dominant uncertainty contributions of the theoretical ratio are $(1.2, 0.78, 0.33) \times 10^{-12}$, originating from the uncertainties of r_d (CODATA 2018), m_d/m_p [11], and QED theory, respectively. The contribution of $u(r_{p,2018})$ is smaller still. The experimental frequency uncertainties are negligible in comparison, once smaller than 0.03 kHz.

Thus, in the context of today's knowledge of fundamental constants, this frequency ratio directly probes the value of the deuteron charge radius. In contrast, in the ratio f_5/f_1 of two HD^+ frequencies discussed in Ref. [5], the dominant non-experiment uncertainties originate from QED theory and μ_{pd}/m_e .

If the improvements in the uncertainty of r_d and of the mass ratios projected in the previous sections are realized at a moderate level, a different interpretation may result. For

TABLE IX. LSA for the determination of the Rydberg constant and charge radii only. Two MHI transitions with low sensitivity to the mass ratios are considered. The experimental inputs are one frequency of HD^+ (a , transition 6), one frequency of H_2^+ (d , transition 4), and H(1S-2S) and H-D(1S-2S) isotope shift measurements. No input from CODATA 2018 is used in the LSA. The uncertainties of the adjusted constants are saturated when the experimental uncertainties are reduced to 0.003 kHz.

Transitions		u_a, u_d	$u_r(R_\infty)$	$u(r_p)$	$u(r_d)$
a	d	(kHz)	10^{-12}	(fm)	(fm)
6	4	0.1, 0.1	2.5	0.0026	0.0010
6	4	0.01, 0.01	0.63	0.00037	0.00013
6	4	0.003, 0.003	0.58	0.00027	0.000090
6	4	0.001, 0.001	0.58	0.00026	0.000085
CODATA 2018			1.9	0.0019	0.00074

TABLE X. LSA for the determination of five fundamental constants from three MHI species and H and D data. The experimental inputs are one frequency of HD^+ (a, transition 3), one frequency of H_2^+ (d, transition 1), one frequency of D_2^+ [f, transition 5, (1, 0) \rightarrow (3, 2)], and H(1S-2S) and H-D(1S-2S) measurements. No input from CODATA 2018 is used in the LSA. The last two scenarios are computed for QED theory uncertainties 1×10^{-12} , a factor 8 smaller than elsewhere in this work. For both levels of theory uncertainty, the uncertainties of the adjusted constants saturate when the experimental uncertainties reach 0.003 kHz. A correlation coefficient of 0.99 between transitions a-f and d-f has been assumed.

Transitions			u_a, u_d, u_f	$u_r(\mu_{pd}/m_e)$	$u_r(m_p/m_e)$	$u_r(R_\infty)$	$u(r_p)$	$u(r_d)$
a	d	f	(kHz)	(10^{-12})	(10^{-12})	(10^{-12})	(fm)	(fm)
3	1	5	0.6, 0.2, 0.2	19	19	5.9	0.0063	0.0025
3	1	5	0.03, 0.03, 0.03	18	19	1.5	0.0015	0.00060
3	1	5	0.003, 0.003, 0.003	18	19	1.5	0.0014	0.00056
3	1	5	0.03, 0.03, 0.03	2.6	2.7	0.79	0.00055	0.00022
3	1	5	0.003, 0.003, 0.003	2.6	2.7	0.63	0.00020	0.000085
CODATA 2018				46	60	1.9	0.0019	0.00074

improvements by factors of 7, the uncertainty of the theoretical ratio (22), approximately 3×10^{-13} , would be dominated by today's QED uncertainty. Then the comparison of experimental and calculated ratios would imply a test of quantum physics at this noteworthy level.

F. Three species

We briefly discuss the scenario of three species that form a closed triad, i.e., having only two distinct nuclei. We choose the nonradioactive triad H_2^+ , D_2^+ , and HD^+ . We consider only transitions between low-lying vibrational levels, for which the QED contributions are more easily computable.

As can be seen from Table X, data row 2, using one transition per species, already for the current theory uncertainty and assuming a 20-fold improvement of experimental uncertainty compared to today, m_p/m_e , the Rydberg constant, and the proton and deuteron charge radii would be obtainable with competitive uncertainties, without using muonic hydrogen data as input data.

Moreover, a putative improvement in QED theory uncertainty by a factor 8 would result in levels substantially below CODATA 2018 for all five fundamental constants. In the last scenario of the table, the fractional uncertainty $u_r(m_d/m_e) \simeq 0.7 \times 10^{-12}$.

IV. DISCUSSION AND CONCLUSION

Here we derived two main results. First, it is in principle possible to determine mass ratios vastly more accurately than known today (CODATA 2018). This could be accomplished by, for example, measuring five MHI transitions with uncertainty at the 1-Hz level. The set of transitions should include transitions between highly excited vibrational levels.

Second, also the Rydberg constant and charge radii can in principle be determined more accurately than known today, provided that future MHI spectroscopy data are combined with already available H and D spectroscopy data. Data on the charge radii from muonic hydrogen spectroscopy are not required. The radii values are adjusted to the MHI, H and D data.

In order to arrive at the above conclusions, we performed two different analyses. The first is an analytical model that was kept simple in order to highlight that one can take advantage of the correlated theory uncertainty for different transitions. The number of experimental transition data considered was kept small and equal to the number of unknown parameters to be determined in a particular scenario. We emphasized that in order to obtain accurate mass ratios, precise *a priori* knowledge of the charge radii (from muonic hydrogen spectroscopy) is not essential. In this model, the values of the charge radii are fitted to the data, always in conjunction with the QED corrections, in the form of the quantity $\Delta_{\text{nuc,QED}}$. If, on the other hand, one would take into account the muonic hydrogen spectroscopy charge radii, the QED corrections Δ_{QED} and the higher-order nuclear size corrections for the proton and the deuteron $\Delta_{\text{nuc,ho}}$ could be obtained separately, from Eqs. (15) and (16).

Within the analytical model we also showed that if more than one MHI species is measured, it is in principle possible to obtain the differences of squared charge radii of a proton, deuteron, and triton, with uncertainties comparable to or smaller than CODATA 2018, using data from MHI spectroscopy only.

The second analysis was a LSA. It has the advantage of being more flexible and powerful, for two reasons. First, it allows one to take into account partial correlations of the theory uncertainties. Second, one can include fundamental constants results and/or data and theory from other systems. Such inclusion is extremely favorable, as is evident from the comparison of Tables VII and VIII. It is then that an impressive improvement of accuracy of the five fundamental constants becomes possible in principle. If the projected fractional uncertainty 6×10^{-14} for the proton-electron mass ratio would be achieved, this would be the most accurately determined fundamental constant, topping the electron g factor.

We highlight that one LSA scenario (Table X) consists of just one highly accurate measurement (10-Hz uncertainty level) on each member of the H_2^+ - HD^+ - D_2^+ triad, in combination with H and D data. This furnishes uncertainties competitive with CODATA 2018 for the five fundamental constants. Notably, the three vibrational transitions do not need to involve large vibrational quantum numbers ν . Thus, the

computation of the theoretical frequencies with the assumed uncertainty 8×10^{-12} will be possible using the already available QED theory techniques.

In the presented LSAs, we only considered scenarios involving three of the six MHIs, HD^+ , H_2^+ , and D_2^+ , but obviously the treatment could be extended to MHIs that contain the triton. We expect that its properties can in principle also be determined with similar uncertainties as for the proton and the deuteron in the considered scenario.

Many scenarios relied on vibrational transitions between levels of large v . We caution that it will be challenging to perform the *ab initio* computation of the corresponding transition frequencies at an uncertainty level of 8×10^{-12} . It is especially the Bethe logarithm that is challenging to compute with sufficient accuracy [23].

Even if the measurement scenarios we have considered allow us to (partially) circumvent limitations associated with QED theory uncertainties, it remains beneficial to improve the theory further, as shown, for example, by the last two lines of Table X. This could be achieved through computation of higher-order corrections to the one-loop self-energy and two-loop corrections that are currently the largest sources of theoretical uncertainty [6], but also by recomputing in a three-body approach some corrections previously calculated in the adiabatic approximation, which would increase the correlations between uncertainties of different transition frequencies (see the discussion in Sec. IB).

In order to achieve the mentioned impressive uncertainties, we considered experimental frequency uncertainties (systematic and statistical combined) as small as 1 Hz, corresponding to fractional frequency uncertainties in the 10^{-15} range. Such levels appear achievable, as our earlier analyses have shown [31,32].

Concerning the experimental feasibility of measuring a hot-band transition frequency, we point out that in HD^+ a rovibrational level with $v = 9$ has a lifetime on the order of 10 ms. This is long enough to allow preparation of a MHI in this level using, e.g., Rabi flopping. The spectroscopic excitation should follow within a time interval of order 1 ms. In the homonuclear MHI, the lifetime of all excited vibrational levels is of the order of days (see Ref. [11] for observations) and so the spectroscopy can take place after a longer wait time and with slower rate.

In H_2^+ , the spectroscopy can be performed on electric quadrupole ($E2$) transitions [33]. Recently, a rovibrational transition has been observed [16], demonstrating feasibility. Transitions to be addressed in future work would likely be those with a small difference $v' - v$, in order to achieve sufficiently high Rabi frequency with available laser sources. Among transitions having $v' - v = 2$, $(12, 0) \rightarrow (14, 2)$ at

46 THz is one with positive-mass-ratio sensitivity, while $(9, 0) \rightarrow (11, 2)$ at 68 THz has suppressed mass-ratio sensitivity. The $E2$ transitions are also suitable for the vibrational spectroscopy of D_2^+ and have been discussed theoretically in detail [34].

In this work we also emphasized that powerful tests of consistency of experimental values obtained from different experiments may be performed; e.g., r_p^2 and r_d^2 obtained from H_2^+ and HD^+ must be consistent with the values obtained from the triad of D_2^+ , HT^+ , and DT^+ . Such tests could be very important in order to uncover overlooked systematic shifts and enhance confidence in the results.

The proposed approach leads to more accurate mass ratios via comparison between experiment and theory prediction. The values of these constants are functions of the forces assumed to act between the particles contained in the MHI. Consequently, the approach may also lead to more sensitive searches for beyond-standard-model (BSM) forces between the particles and more accurate tests of their wave properties, topics that have been explored in recent studies [1,2,5,35]. The BSM signatures could appear in values of the obtained Rydberg constant, mass ratios, or differences of squared radii, which do not agree with measurements on the electronic and muonic hydrogen isotopes and direct mass measurements. One simple example of a BSM physics test is the comparison of the charge radii from Table VIII, obtained from MHIs and electronic H and D, with those obtained from muonic H and D. The latter values were derived assuming conventional QED for the muon-radiation field interaction and for the muon-nucleus interaction. Any discrepancy between the two sets of results could hint at BSM forces.

A BSM electron-nucleus interaction that depends on the nuclear composition could be probed using data obtained only from MHIs (as a violation of the relationship (3) in [26]) or as inconsistent mass-ratio values obtained from different MHI species. Such effects could also be tested in a LSA where the energy shifts induced by hypothetical BSM interactions are included and parameters describing these interactions are adjusted [5,35].

ACKNOWLEDGMENTS

We thank V. I. Korobov for putting at our disposal his codes for the computation of the nonrelativistic energies and expectation values. S.S. thanks M. Schenkel, I. Kortunov, and C. Wellers for discussions and S. Alighanbari for discussions and comments on the text. This work received funding from the European Research Council under the European Union's Horizon 2020 research and innovation program through Grant Agreement No. 786306, PREMOL (S.S.).

- [1] S. Alighanbari, G. S. Giri, F. L. Constantin, V. I. Korobov, and S. Schiller, Precise test of quantum electrodynamics and determination of fundamental constants with HD^+ ions, *Nature (London)* **581**, 152 (2020).
- [2] M. Germann, S. Patra, J.-Ph. Karr, L. Hilico, V. I. Korobov, E. J. Salumbides, K. S. E. Eikema, W. Ubachs, and J. C. J. Koelemeij, Three-body QED test and fifth-force constraint from

vibrations and rotations of HD^+ , *Phys. Rev. Res.* **3**, L022028 (2021).

- [3] S. Patra, M. Germann, J.-Ph. Karr, M. Haidar, L. Hilico, V. I. Korobov, F. M. J. Cozijn, K. S. E. Eikema, W. Ubachs, and J. C. J. Koelemeij, Proton-electron mass ratio from laser spectroscopy of HD^+ at the part-per-trillion level, *Science* **369**, 1238 (2020).

- [4] I. V. Kortunov, S. Alighanbari, M. G. Hansen, G. S. Giri, V. I. Korobov, and S. Schiller, Proton-electron mass ratio by high-resolution optical spectroscopy of ion ensembles in the resolved-carrier regime, *Nat. Phys.* **17**, 569 (2021).
- [5] S. Alighanbari, I. V. Kortunov, G. S. Giri, and S. Schiller, Test of charged baryon interaction with high-resolution vibrational spectroscopy of molecular hydrogen ions, *Nat. Phys.* **19**, 1263 (2023).
- [6] V. I. Korobov and J.-Ph. Karr, Rovibrational spin-averaged transitions in the hydrogen molecular ions, *Phys. Rev. A* **104**, 032806 (2021).
- [7] J.-Ph. Karr and J. C. J. Koelemeij, Extraction of spin-averaged rovibrational transition frequencies in HD^+ for the determination of fundamental constants, *Mol. Phys.* **121**, e2216081 (2023).
- [8] F. Köhler, S. Sturm, A. Kracke, G. Werth, W. Quint, and K. Blaum, The electron mass from g -factor measurements on hydrogen-like carbon $^{12}\text{C}^{5+}$, *J. Phys. B: At. Mol. Opt. Phys.* **48**, 144032 (2015).
- [9] F. Heiße, S. Rau, F. Köhler-Langes, W. Quint, G. Werth, S. Sturm, and K. Blaum, High-precision mass spectrometer for light ions, *Phys. Rev. A* **100**, 022518 (2019).
- [10] S. Rau, F. Heiße, F. Köhler-Langes, S. Sasidharan, R. Haas, D. Renisch, C. E. Düllmann, W. Quint, S. Sturm, and K. Blaum, Penning trap mass measurements of the deuterium and the HD^+ molecular ion, *Nature (London)* **585**, 43 (2020).
- [11] D. J. Fink and E. G. Myers, Deuteron-to-proton mass ratio from simultaneous measurement of the cyclotron frequencies of H_2^+ and D^+ , *Phys. Rev. Lett.* **127**, 243001 (2021).
- [12] J.-Ph. Karr, L. Hilico, J. C. J. Koelemeij, and V. I. Korobov, Hydrogen molecular ions for improved determination of fundamental constants, *Phys. Rev. A* **94**, 050501(R) (2016).
- [13] P. J. Mohr and B. N. Taylor, CODATA recommended values of the fundamental physical constants: 1998, *Rev. Mod. Phys.* **72**, 351 (2000).
- [14] E. Tiesinga, P. J. Mohr, D. B. Newell, and B. N. Taylor, CODATA recommended values of the fundamental physical constants: 2018, *Rev. Mod. Phys.* **93**, 025010 (2021).
- [15] S. Schiller and V. I. Korobov, Canceling spin-dependent contributions and systematic shifts in precision spectroscopy of molecular hydrogen ions, *Phys. Rev. A* **98**, 022511 (2018).
- [16] M. R. Schenkel, S. Alighanbari, and S. Schiller, Laser spectroscopy of a rovibrational transition in the molecular hydrogen ion H_2^+ , *Nat. Phys.* **20**, 383 (2024).
- [17] S. Schiller and V. Korobov, Test of time dependence of the electron and nuclear masses with ultracold molecules, *Phys. Rev. A* **71**, 032505 (2005).
- [18] J.-Ph. Karr and L. Hilico, High accuracy results for the energy levels of the molecular ions H_2^+ , D_2^+ and HD^+ , up to $J = 2$, *J. Phys. B: At. Mol. Opt. Phys.* **39**, 2095 (2006).
- [19] D. T. Aznabayev, A. K. Bekbaev, and V. I. Korobov, Leading-order relativistic corrections to the rovibrational spectrum of H_2^+ and HD^+ molecular ions, *Phys. Rev. A* **99**, 012501 (2019).
- [20] V. I. Korobov, L. Hilico, and J.-Ph. Karr, Fundamental transitions and ionization energies of the hydrogen molecular ions with few ppt uncertainty, *Phys. Rev. Lett.* **118**, 233001 (2017).
- [21] V. I. Korobov, L. Hilico, and J.-Ph. Karr, Theoretical transition frequencies beyond 0.1 ppb accuracy in H_2^+ , HD^+ , and antiprotonic helium, *Phys. Rev. A* **89**, 032511 (2014).
- [22] J.-Ph. Karr, L. Hilico, and V. I. Korobov, One-loop vacuum polarization at $m\alpha^7$ and higher orders for three-body molecular systems, *Phys. Rev. A* **95**, 042514 (2017).
- [23] V. I. Korobov and Z.-X. Zhong, Bethe logarithm for the H_2^+ and HD^+ molecular ions, *Phys. Rev. A* **86**, 044501 (2012).
- [24] Z.-X. Zhong, W.-P. Zhou, and X.-S. Mei, Spin-averaged effective Hamiltonian of orders $m\alpha^6$ and $m\alpha^6(m/M)$ for hydrogen molecular ions, *Phys. Rev. A* **98**, 032502 (2018).
- [25] V. I. Korobov, Ro-vibrational states of H_2^+ . Variational calculations, *Mol. Phys.* **116**, 93 (2018).
- [26] See Supplemental Material at <http://link.aps.org/supplemental/10.1103/PhysRevA.109.042825> for discussion of several additional measurement scenarios using the analytical model described in Sec. II.
- [27] C. G. Parthey, A. Matveev, J. Alnis, B. Bernhardt, A. Beyer, R. Holzwarth, A. Maistrou, R. Pohl, K. Predehl, T. Udem, T. Wilken, N. Kolachevsky, M. Abgrall, D. Rovera, C. Salomon, P. Laurent, and T. W. Hänsch, Improved measurement of the hydrogen $1s-2s$ transition frequency, *Phys. Rev. Lett.* **107**, 203001 (2011).
- [28] A. Matveev, C. G. Parthey, K. Predehl, J. Alnis, A. Beyer, R. Holzwarth, T. Udem, T. Wilken, N. Kolachevsky, M. Abgrall, D. Rovera, C. Salomon, P. Laurent, G. Grosche, O. Terra, T. Legero, H. Schnatz, S. Weyers, B. Altschul, and T. W. Hänsch, Precision measurement of the hydrogen $1s-2s$ frequency via a 920-km fiber link, *Phys. Rev. Lett.* **110**, 230801 (2013).
- [29] C. G. Parthey, A. Matveev, J. Alnis, R. Pohl, T. Udem, U. D. Jentschura, N. Kolachevsky, and T. W. Hänsch, Precision measurement of the hydrogen-deuterium $1s-2s$ isotope shift, *Phys. Rev. Lett.* **104**, 233001 (2010).
- [30] T. Schneider, B. Roth, H. Duncker, I. Ernsting, and S. Schiller, All-optical preparation of molecular ions in the rovibrational ground state, *Nat. Phys.* **6**, 275 (2010).
- [31] S. Schiller, D. Bakalov, and V. I. Korobov, Simplest molecules as candidates for precise optical clocks, *Phys. Rev. Lett.* **113**, 023004 (2014).
- [32] J.-Ph. Karr, H_2^+ and HD^+ : Candidates for a molecular clock, *J. Mol. Spectrosc.* **300**, 37 (2014).
- [33] V. I. Korobov, P. Danev, D. Bakalov, and S. Schiller, Laser-stimulated electric quadrupole transitions in the molecular hydrogen ion H_2^+ , *Phys. Rev. A* **97**, 032505 (2018).
- [34] P. Danev, D. Bakalov, V. I. Korobov, and S. Schiller, Hyperfine structure and electric quadrupole transitions in the deuterium molecular ion, *Phys. Rev. A* **103**, 012805 (2021).
- [35] C. Delaunay, J.-Ph. Karr, T. Kitahara, J. C. J. Koelemeij, Y. Soreq, and J. Zupan, Self-consistent extraction of spectroscopic bounds on light new physics, *Phys. Rev. Lett.* **130**, 121801 (2023).

**Prospects for the determination of fundamental constants with
beyond-state-of-the-art uncertainty using molecular hydrogen ion
spectroscopy**

S. Schiller*

*Institut für Experimentalphysik, Heinrich-Heine-
Universität Düsseldorf, 40225 Düsseldorf, Germany*

J.-Ph. Karr^{1,2}

*¹Laboratoire Kastler Brossel, Sorbonne Université, CNRS, ENS,
Université PSL, Collège de France, 4 Place Jussieu, 75005 Paris,
France; ²Université d'Evry-Val d'Essonne, Université Paris-Saclay,
Boulevard François Mitterrand, 91000 Evry, France*

SUPPLEMENTAL MATERIAL

ANALYTICAL MODEL: OTHER SCENARIOS

In this Supplemental Material, we investigate the achievable accuracy of fundamental constants determinations in several measurement scenarios using the analytical model described in Sec. II of the main paper. The first three scenarios discussed below are also addressed in the main paper (see Sec. III.1, III.2 III.6) using a more rigorous approach relying on least-squares adjustments.

1. Two transitions in one species

We first consider the case, when only two transitions have been measured, $f_a^{(\text{expt})}$ and $f_b^{(\text{expt})}$. They have respective experimental uncertainties $u_a = u(f_a^{(\text{expt})})$ and $u_b = u(f_b^{(\text{expt})})$, which we assume to be uncorrelated. The uncertainty of the Rydberg constant is taken as given, with value $u(\Delta_{h,2018}) = u_r(R_{\infty,2018})$. Solving the equations

$$f_a^{(\text{expt})} = f_a^{(\text{theor})}, f_b^{(\text{expt})} = f_b^{(\text{theor})},$$

one immediately obtains $\Delta_{m,\mu}$, and it has an uncertainty

$$u(\Delta_{m,\mu})^2 = (s_b V_a - s_a V_b)^{-2} \times \left(V_b^2 \left(\frac{u_a}{2c R_{\infty}} \right)^2 + V_a^2 \left(\frac{u_b}{2c R_{\infty}} \right)^2 + \right. \quad (1)$$

$$\left. ((f_{\text{nr,a.u.})_a V_b - (f_{\text{nr,a.u.})_b V_a})^2 u(\Delta_h)^2 \right), \quad (2)$$

with the notations $V_j = (\langle V_{\delta,12} \rangle_{v',N'} - \langle V_{\delta,12} \rangle_{v,N})_j$, $s_j = \partial(f_{\text{nr,a.u.})_j} / \partial(\mu_{12}/m_e)$ for the two transitions $j = a, b$. The analogous expression for $\Delta_{\text{nuc,QED}}$ will be omitted for brevity.

Table I shows numerical examples of the uncertainties achievable for different two-transition scenarios in HD⁺. One main result is that it is favourable to have a positive-sensitivity transition result available (transition 5). Compared to the case where no such result is available, one obtains the same uncertainty $u(\Delta_{m,\mu})$ with a tenfold worse experimental frequency uncertainty. Alternatively, for the same experimental frequency uncertainty, in case of availability one obtains a five times smaller uncertainty $u(\Delta_{m,\mu})$. As eq. (1) indicates, the attainable uncertainty for the reduced mass ratio μ_{12}/m_e is limited by the uncertainty $u(\Delta_{h,2018})$ of the Rydberg constant, to a value $\text{Min}(u(\Delta_{m,\mu})) \approx 6 \times 10^{-10}$. This is a factor 100

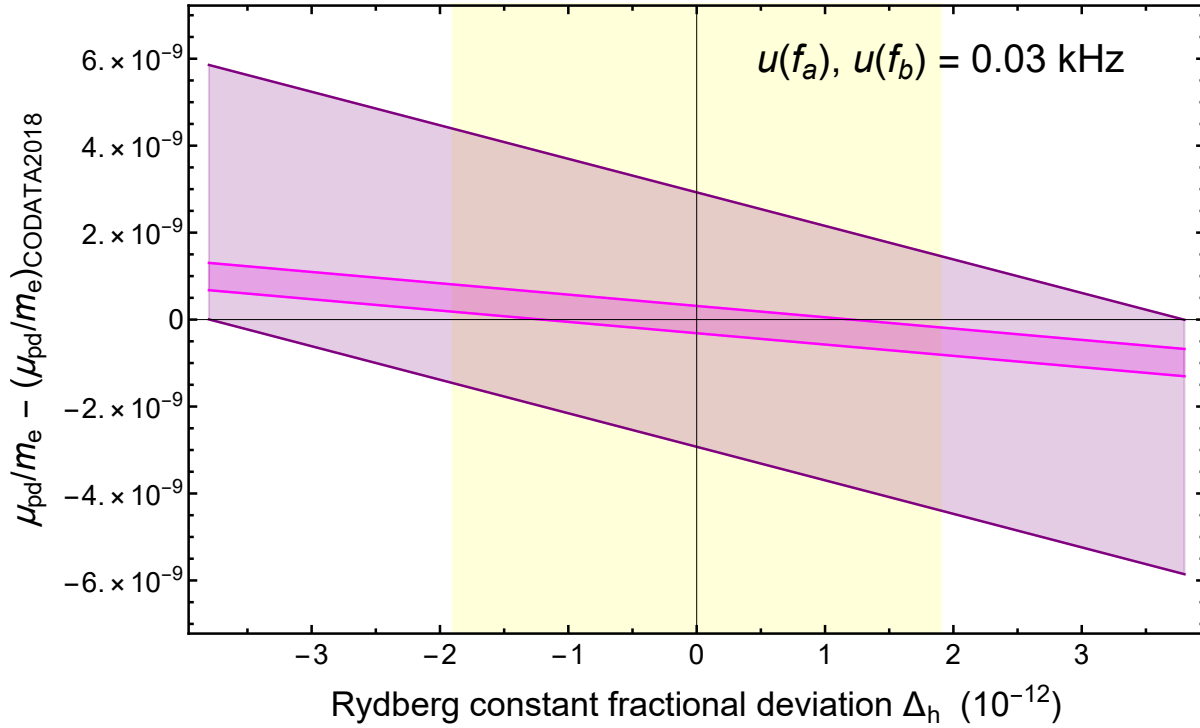


FIG. 1. Proposed determination of the mass ratio μ_{pd}/m_e from measurements of a frequency pair (f_a, f_b) in HD^+ . Two cases are shown, in purple and magenta. Purple: transitions $a: (v = 0, N = 0) \rightarrow (v' = 5, N' = 1)$ and $b: (0, 3) \rightarrow (9, 3)$. Magenta: transitions $a: (0, 0) \rightarrow (5, 1)$ and $b: (9, 1) \rightarrow (18, 0)$. The widths of the magenta and purple bands are due to the assumed experimental frequency uncertainties $u(f_a), u(f_b)$. The yellow band indicates today's (CODATA 2018) uncertainty of the Rydberg constant. The slope and width of a band together with the width of the yellow band determines the uncertainty of μ_{pd}/m_e . The magenta case is more favourable.

smaller than the CODATA 2018 uncertainty and a factor ≈ 40 smaller than the uncertainty reported to date from MHI spectroscopy, $u([\Delta_{m,\mu}]_{\text{expt,HD}^+}) \simeq 2.5 \times 10^{-8}$. Achieving the limit $\text{Min}(u(\Delta_{m,\mu}))$ requires the experimental uncertainties u_a, u_b to be approximately 0.03 kHz. Note that this level is much more stringent than the transition frequency uncertainty related to the Rydberg constant uncertainty, $u(\Delta_{h,2018}) \times f_{a,b} \simeq 0.4 \text{ kHz}$. Figure 1 displays the advantage of using both a negative-sensitivity transition and a positive-sensitivity transition (magenta band).

The last line in Table I reports the result for the experimentally measured transitions 3 and 4 when their actually achieved experimental uncertainties are assumed. The com-

puted uncertainty $u(\Delta_{m,\mu}) \simeq 5.5 \times 10^{-8}$ is higher than the already achieved uncertainty $u([\Delta_{m,\mu}]_{\text{expt,HD}^+})$. This is so because in the table, $\Delta_{\text{nuc,QED}}$ was adjusted, while in the reported works, it was not; $\Delta_{\text{nuc}}(\text{HD}^+)$ and Δ_{QED} were set to be zero with uncertainties as quoted above.

a	b	$ s_b V_a - s_a V_b ^{-1}$ (10^6)	u_a, u_b (kHz)	analytical model			LSA	
				contrib. to $u(\Delta_{m,\lambda})$ from ... u_a, u_b (10^{-10})	$u(\Delta_{m,\lambda})$ (10^{-10})	$u(\Delta_{\text{HD}^+})$	$u(\Delta_{m,\lambda})$ (10^{-10})	
2	3	75	0.3	1500	23	1500	2.3	233
2	3	75	0.03	150	23	150	0.26	180
3	4	8.3	0.3	290	15	290	0.43	202
3	4	8.3	0.03	29	15	33	0.12	136
3	5	1.4	0.3	31	4.9	32	0.11	43
3	5	1.4	0.03	3.1	4.9	5.9	0.094	29
3	6	2.2	0.3	53	7.4	54	0.12	91
3	8	3.0	0.3	80	9.4	80	0.14	125
3	4	8.3	{0.6, 0.46}	550	15	550	0.78	240
CODATA 2018						560		560

TABLE I. Examples of mass ratio determination by measuring a pair of transitions a and b in HD^+ . In the analytical model no other data is used. The absolute uncertainty of $\lambda = \mu_{pd}/m_e$ is given in column 7 as $u(\Delta_{m,\lambda})$, and column 8 is the uncertainty of the fitted nuclear plus QED correction parameter. In the LSA procedure (last column), non-perfect theory uncertainty correlations are taken into account and, in addition to the two HD^+ data, also the CODATA 2018 values of R_∞ , r_p , r_d , see main paper, sec. III.1. The last data row considers the scenario of two already performed experiments. We used the abbreviation $\Delta_{\text{HD}^+} = \Delta_{\text{nuc,QED}}(\text{HD}^+)$.

2. Three transitions in one species

With three or more transitions available, besides $\Delta_{m,\mu}$ and $\Delta_{\text{nuc,QED}}$, also the Rydberg constant can be determined. Explicit expressions for $u(\Delta_{m,\mu})$, $u(\Delta_{\text{nuc,QED}})$ and $u(\Delta_h)$ can easily be derived, but will not be displayed here. Table II shows numerical results for various combinations of transitions. For given experimental frequency uncertainties u_a , u_b and u_c , those combinations containing the positive-mass-sensitivity transition 5 yield reduced uncertainties. We find that the three uncertainties $u(\Delta_{m,\mu})$, $u(\Delta_{\text{nuc,QED}})$, and $u(\Delta_h)$ drop continuously with decreasing u_a , u_b , and u_c . In particular, the uncertainty of $\Delta_{m,\mu}$ drops below the minimum achievable for the case of only two measured transitions. For example, $u(\Delta_{m,\mu}) \simeq 4 \times 10^{-11}$, one order lower than for the case of two transitions only, is obtained if the experimental frequency uncertainties are 1 Hz. For such experimental accuracy, the uncertainty of the Rydberg constant is determined with ten-fold lower uncertainty than CODATA 2018's uncertainty.

We point out that the QED contribution parameter $\Delta_{\text{nuc,QED}}$ is then determined with uncertainty 0.01, i.e. approximately 30 times smaller than today's estimate. For an individual transition this corresponds to a theoretical uncertainty of e.g. $\simeq 60$ Hz for transition 3, a much larger value than the assumed experimental uncertainty. The reason for the different magnitude is the correlation between the QED deviation function $\langle V_{\delta,12} \rangle_{v',N'} - \langle V_{\delta,12} \rangle_{v,N}$ and the transition frequency $f(v, N \rightarrow v', N')$.

3. Three Species

Suppose precision spectroscopy is also performed on D_2^+ . Data from it alone will provide the deuteron-electron mass ratio m_d/m_e , and thus a consistency check is possible with the independent value obtained from combined HD^+ and H_2^+ measurements. Furthermore, $\Delta_{\text{nuc,QED}}(\text{D}_2^+)$ is obtained. Since

$$\Delta_{\text{nuc,QED}}(\text{D}_2^+) = \alpha^{-5} (2\pi/3) a_0^{-2} \frac{1}{2} \times 2 \Delta(r_d^2) + \Delta_{\text{QED}} + 2\Delta_{\text{nuc,h.o.}}(d),$$

the comparison with eqs. (16,17) (main paper) shows that

$$\Delta_{\text{nuc,QED}}(\text{D}_2^+) = 2\Delta_{\text{nuc,QED}}(\text{HD}^+) - \Delta_{\text{nuc,QED}}(\text{H}_2^+). \quad (3)$$

Transitions			u_a, u_b, u_c (kHz)	contrib. to $u(\Delta_{m,\lambda})$ from ...			$u(\Delta_{m,\lambda})$ (10^{-10})	$u(\Delta_h)$ (10^{-12})	$u(\Delta_{\text{nuc,QED}})$
a	b	c		u_a (10^{-10})	u_b (10^{-10})	u_c (10^{-10})			
2	3	4	{0.15, 0.6, 0.46}	1300	700	2600	3000	330	20
3	4	5	{0.3, 0.3, 0.3}	98	39	81	130	55	2.7
3	4	5	{0.03, 0.03, 0.03}	9.8	3.9	8.1	13	5.5	0.27
3	4	5	{0.01, 0.01, 0.01}	3.3	1.3	2.7	4.4	1.8	0.091
3	4	5	{0.003, 0.003, 0.003}	0.98	0.39	0.81	1.3	0.55	0.027
3	4	5	{0.001, 0.001, 0.001}	0.33	0.13	0.27	0.44	0.18	0.0091
3	5	6	{0.003, 0.003, 0.003}	0.15	0.85	0.79	1.2	0.41	0.020
3	5	8	{0.003, 0.003, 0.003}	0.24	0.64	0.55	0.88	0.31	0.016
3	6	7	{0.003, 0.003, 0.003}	0.27	10	5.5	12	3.0	0.16
3	6	8	{0.003, 0.003, 0.003}	0.47	2.1	1.9	2.9	0.70	0.037
CODATA 2018							560	1.9	

TABLE II. Analytical model: examples of the determination of both the reduced mass $\lambda = \mu_{pd}/m_e$ and the Rydberg constant by measuring three transitions in HD^+ . In column 8, $u(\Delta_{m,\lambda})$ is the absolute uncertainty of λ . In column 9, $u(\Delta_h) = u_r(R_\infty)$ is the fractional uncertainty of the fitted Rydberg constant. The first case in the table (data row 1) considers the three rovibrational transitions measured to date. In this case, because the Rydberg constant is among the fitted constants, no competitive uncertainty is obtained for the fitted mass ratio.

Thus, data from D_2^+ does not provide new information concerning the radii. One cannot simultaneously determine the unknown QED contribution and obtain the radii r_p, r_d *individually*. Still, this expression provides a very important consistency check with the result from combined $\text{H}_2^+, \text{HD}^+$ measurements. The three-species scenario is also analyzed in Sec. III.6 of the main paper, this time including data from atomic hydrogen spectroscopy. A different conclusion is then reached.

4. Including one triton-containing species

If e.g. HT^+ is measured, apart from μ_{pt}/m_e , the fit also yields $\Delta_{\text{nuc,QED}}(\text{HT}^+)$, which is given by

$$\Delta_{\text{nuc,QED}}(\text{HT}^+) = \alpha^{-5}(2\pi/3)a_0^{-2}\frac{1}{2} \times \Delta(r_p^2 + r_t^2) + \Delta_{\text{QED}} + \Delta_{\text{nuc,h.o.}}(t).$$

The recoil correction of this species is assumed to be treated in the same way as described earlier. One can combine this with the H_2^+ results, eq. (16) in the main paper, to obtain $\Delta(r_t^2) - \Delta(r_p^2)$ with minimum uncertainty given by the uncertainty of $\Delta_{\text{nuc,h.o.}}(t)$. The latter is dominated by the triton polarizability correction $E_{\text{pol}}^{(5)}$, for which no calculation has been reported, although the electric dipole polarizability of the triton was calculated in [1]. One may adopt the estimate given in [2]:

$$E_{\text{pol}}^{(5)} \approx -\frac{E_{\text{fms}}}{1000} \pm 100\%,$$

where E_{fms} is the leading-order finite-nuclear-size correction. This yields

$$\begin{aligned} u(\delta f_{\text{nuc,h.o.}}(t)) &= \frac{1}{1000} \times 2cR_\infty \frac{2\pi}{3} \left(\frac{r_t}{a_0}\right)^2 \frac{1}{2} (\langle V_{\delta,pt} \rangle_{v',N'} - \langle V_{\delta,pt} \rangle_{v,N}), \\ &= 7.6 \text{ kHz} \times (\langle V_{\delta,pt} \rangle_{v',N'} - \langle V_{\delta,pt} \rangle_{v,N}); \\ u(\Delta_{\text{nuc,h.o.}}(t)) &= \frac{1}{1000} \times \alpha^{-5} \frac{2\pi}{3} \left(\frac{r_t}{a_0}\right)^2 \frac{1}{2}. \end{aligned}$$

This implies that $\Delta(r_t^2) - \Delta(r_p^2)$ could then be deduced with an uncertainty of about $r_t^2/1000 \simeq 0.003 \text{ fm}^2$, which would already represent a considerable improvement compared to today's experimental uncertainty. The current triton radius value is $r_t^{(\text{expt})} = 1.755(86) \text{ fm}$ from electron scattering experiments [3]. Its absolute uncertainty is substantially larger than that of r_p and r_d , eq. (3) in the main paper. Calculation of the triton polarizability contribution would allow reaching even higher precision.

In nuclear physics, the triton is a nucleus of substantial interest. Its *point* charge radius δr_C , that is related to the charge radius, can be computed using effective field theory [4, 5] with competitive uncertainty. A recent calculation of $\delta r_C^{(\text{theory})}$ yields, when combined with the experimental ^3He charge radius, a preliminary value $r_t = 1.773(9) \text{ fm}$ [5]. Precision data on H_2^+ and HT^+ could verify this prediction and also future, much improved predictions. Thus, HT^+ spectroscopy could be an alternative to future laser spectroscopy of atomic tritium [6].

5. The group of heteronuclear MHI

If DT^+ is also included to complete the triad of heteronuclear MHI, one will obtain μ_{dt}/m_e and $\Delta_{\text{nuc,QED}}(\text{DT}^+)$, given by

$$\alpha^5 \Delta_{\text{nuc,QED}}(\text{DT}^+) = (2\pi/3)a_0^{-2} \frac{1}{2} \times \Delta(r_d^2 + r_t^2) + \Delta_{\text{QED}} + \Delta_{\text{nuc,h.o.}}(d) + \Delta_{\text{nuc,h.o.}}(t).$$

Combination with the HT^+ result yields

$$\alpha^5 \Delta_{\text{nuc,QED}}(\text{DT}^+) - \alpha^5 \Delta_{\text{nuc,QED}}(\text{HT}^+) = (2\pi/3)a_0^{-2} \frac{1}{2} \times \Delta(r_d^2 - r_p^2) + \Delta_{\text{nuc,h.o.}}(d).$$

This is the same result as eq. (18) in the main paper, obtained from H_2^+ and HD^+ . Similarly, combining DT^+ and HD^+ results one obtains $\Delta(r_t^2 - r_d^2)$ (modulo the higher-order nuclear correction for t). This means that one can in principle obtain the information on the charge radii without performing measurements on the homonuclear ions. Such an approach may have some experimental advantages. Alternatively, one can verify experimentally consistency of independent measurements performed on four different MHI, e.g. H_2^+ , HD^+ , HT^+ , DT^+ .

-
- [1] I. Stetcu, S. Quaglioni, J. L. Friar, A. C. Hayes, P. Navrátil, Electric dipole polarizabilities of hydrogen and helium isotopes, *Phys. Rev. C* 79 (2009) 064001. doi:10.1103/PhysRevC.79.064001.
- [2] V. A. Yerokhin, V. M. Shabaev, Lamb Shift of $n = 1$ and $n = 2$ States of Hydrogen-like Atoms, $1 \leq Z \leq 110$, *Journal of Physical and Chemical Reference Data* 44 (3) (2015) 033103. doi:10.1063/1.4927487.
- [3] A. Amroun, V. Breton, J.-M. Cavedon, B. Frois, D. Goutte, F. Juster, P. Leconte, J. Martino, Y. Mizuno, X.-H. Phan, S. Platchkov, I. Sick, S. Williamson, ^3H and ^3He electromagnetic form factors, *Nuclear Physics A* 579 (1994) 596–626. doi:10.1016/0375-9474(94)90925-3.
- [4] J. Vanasse, Triton charge radius to next-to-next-to-leading order in pionless effective field theory, *Phys. Rev. C* 95 (2017) 024002. doi:10.1103/PhysRevC.95.024002.
- [5] A. Filin, private comm. (2023).
URL <https://indico.uis.no/event/2/contributions/523/>
- [6] S. Schmidt, M. Willig, J. Haack, R. Horn, A. Adamczak, M. A. Ahmed, F. D. Amaro, P. Amaro, F. Biraben, P. Carvalho, T.-L. Chen, L. M. P. Fernandes, T. Graf, M. Guerra, T. W. Hänsch,

M. Hildebrandt, Y.-C. Huang, P. Indelicato, L. Julien, K. Kirch, A. Knecht, F. Kottmann, J. J. Krauth, Y.-W. Liu, J. Machado, M. Marszalek, C. M. B. Monteiro, F. Nez, J. Nuber, D. N. Patel, E. Rapisarda, J. M. F. dos Santos, J. P. Santos, P. A. O. C. Silva, L. Sinkunaite, J.-T. Shy, K. Schuhmann, I. Schulthess, D. Taqqu, J. F. C. A. Veloso, L.-B. Wang, M. Zeyen, A. Antognini, R. Pohl, The next generation of laser spectroscopy experiments using light muonic atoms, *Journal of Physics: Conference Series* 1138 (2018) 012010. doi:10.1088/1742-6596/1138/1/012010.